Theory of coevolution of cytoplasmic male-sterility, nuclear restorer and selfing

Atsushi Yamauchi[1†], Takahiro Yamagishi[1], Ross Booton[2], Arndt Telschow[3], Gaku Kudo[4]

Running title: CMS, restorer and selfing

Journal of Theoretical Biology, 477 (2019) 96–107

DOI: https://doi.org/10.1016/j.jtbi.2019.06.011

[1] Center for Ecological Research, Kyoto University, Hirano 2-509-3, Otsu 520-2113, Japan
[2] School of Public Health, Faculty of Medicine, Imperial College London, Medical School Building, St Mary's Campus, Norfolk Place, London W2 1PG, United Kingdom
[3] Institute for Environmental Systems Research, Osnabrück University, 49069 Osnabrück, Germany
[4] Faculty of Environmental Earth Science, Hokkaido University, Sapporo 060-0810, Japan

[†] (Corresponding author)
Atsushi Yamauchi
Tel: +81-77-549-8259
Fax: +81-77-549-8201
E-mail: a-yama@ecology.kyoto-u.ac.jp

ABSTRACT

Gynodioecy is a sexual polymorphism in angiosperms, where hermaphroditic and female individuals coexist. This is often caused by a cytoplasmic genetic element (CGE) that destroys male functions, which is called cytoplasmic male-sterility (CMS). On the other hand, nuclear genes tend to evolve the ability to restore male function. The coevolutionary process of CMS and the restoration has been studied theoretically. Recently, a theoretical study suggested that these coevolutionary dynamics could be influenced by the rate of selfing within populations, although it assumed that the selfing rate of a population was a fixed parameter. Accordingly, we theoretically study the coevolution of three traits in this paper: CMS, nuclear restorer and selfing rate, in which we hypothesize that selfing evolution can suppress CMS evolution under some conditions. The analysis indicates three significant properties of the system; (1) CMS-restorer evolution can result in bistability under a given selfing rate, (2) the coevolution of three traits can realize intermediate levels of selfing, and (3) the evolution of high levels of selfing is conditionally associated with no CMS and/or no restoration, which may support our hypothesis.

Keywords: gynodioecy, inter-genomic conflict, pollen discounting, pollen limitation, inbreeding depression, cost of restorer

INTRODUCTION

Gynodioecy is a sexual polymorphism in angiosperms, where hermaphroditic and female individuals coexist within a population. Gynodioecy is often caused by a cytoplasmic genetic element (CGE) which destroys male functions, typically through mitochondrial mutants (see review by Hanson (1991)), which is termed cytoplasmic male-sterility (CMS). Lewis (1941) was a pioneer in the theoretical research of CMS evolution in plants. He showed that the CMS cytoplasm can increase in a population if CMS results in an advantage in female fitness, and that a frequency of CMS reaches a stable equilibrium if the female fitness involves a negative frequency dependence. After this, Lloyd (1974) theoretically studied the dynamics of both nuclear- and cytoplasmic-controlling male-sterility, and investigated the effects of self-fertilization on gynodioecy. Lloyd (1975) then extended his previous study by considering inbreeding depression and showed that male-steriles can be maintained in a population when their obligatorily outcrossed progenies have higher fitness than the inbred progeny (from self-fertilization in hermaphrodites).

CGEs are not transmitted to offspring via male gametes, therefore they would evolve male-sterility when CGEs promote the individual female function. On the other hand, the male function can genetically contribute to nuclear transmission via male gametes, which results in the inter-genomic conflict between CGE and nucleus (Burt & Trivers, 2009), by which nuclear restore evolves to recover male function. Incuding this factor, theoretical models were developed to investigate the coevolution between CMS and nuclear restorer allele (Charlesworth & Ganders, 1979). Those early theoretical studies of the coevolution of CMS and nuclear restorer concluded that the final population is fixed for CMS with either restorer fixation (i,e., hermaphrodite) or remains polymorphic for the restorer alleles. In the case with restorer polymorphism, individuals with and without restorer allele develop into hermaphrodite and female, respectively, which corresponds to gynodyoecy in some species, called "nuclear gynodioecy" (NG). In other species, however, both nuclear gene and cytoplasm are responsible for the individual sex determination (Bailey & Delph, 2007b), which is called "nuclear-cytoplasmic gynodioecy" (NCG) (Dornier & Dufay, 2013). In order to explain the role of cytoplasm in determining sexuality, theoretical researchers have included a cost of restoration into the model (Delannay et al., 1981, Charlesworth, 1981, Gouyon et al., 1991, Jacobs & Wade, 2003, McCauley & Bailey, 2009, Bailey & Delph, 2007b, Dufay et al., 2007), which indicated the importance of restoration cost in the stable maintenance of nuclear-cytoplasmic gynodioecy. Theoretical studies have also shown that the restoration cost can contribute to the coexistence of multiple types of resotorer-CMS interactions in a population (Gouyon et al., 1991, Maurice et al., 1993, Bailey et al., 2003). Furthermore, Gouyon et al. (1991) and Dufay et al. (2007) showed that when both restorer and CMS are accompanied by costs, a continuous oscillation with a limit cycle is possible in a gynodioecious population. These theoretical studies of restoration cost have revealed evolutionary dynamics of nuclear-cytoplasmic gynodioecy, although the recent studies tended to focus on self-incompatible species (except for a discussion by Jacobs and Wade (2003)), thereby ignoring effects of selfing that were considered in earlier published studies (Charlesworth, 1981, Delannay et al., 1981).

It should be remarked that the theoretical studies of gynodioecy have generally adopted one critical assumption: a negative correlation between female fitness and female frequency in the population, which is typically derived from the process of pollination. This assumption is based on the principle of "pollen limitation" (Knight et al., 2005), by which there is a positive correlation between the fertilization rate of ovules and the density of male organs in the population, so that fertilization is restricted by the frequencies of male-sterile individuals. This limitation results in a negative frequency-dependence in female fitness, which can stabilize gynodioecy (Maurice & Fleming, 1995). Importantly, this process may be enhanced in the presence of self-fertilization in hermaphrodites, where the total exportation of pollen is limited due to individual self-consumption (Charlesworth, 1980). The reduction of pollen exportation by a preceding self-pollination is called "pollen discounting" (Harder & Wilson, 1998, Porcher & Lande, 2005a). Through the combination of pollen limitation and discounting, selfing of hermaphrodites can negatively influence the fitness of CMS females by restricting fertilization in outbreeding. It should also be remarked that this also affects the fitness of hermaphrodites with autogamous selfing, because selfing ability without the help of pollinators ensures the fertilization of their own ovules even under severe pollen limitation, which is called "reproductive assurance" (Sicard & Lenhard, 2011). Theoretical studies have found that in a gynodioecious population, autogamous selfing can be an effective assurance for hermaphrodite reproduction (Maurice & Fleming, 1995). Indeed, Lahiani et al. (2015) empirically measured seed production, strength of pollen limitation, and the selfing rates of hermaphroditic individuals in both female-biased and hermaphrodite-biased gynodioecious populations. They clearly indicated that selfing can be a reproductive assurance, by which hermaphrodites are more tolerant to pollen limitation than females especially in female-biased populations.

Despite an expectation of a significant effect of selfing, it has rarely been included within theoretical studies of CMS-restorer coevolution. Charlesworth (1981) initially investigated this issue, although the model did not include any cost of restoration. Delannay et al. (1981) and Jacobs and Wade (2003) clarified selection in CMS-restorer coevolution with selfing in the presence of a restoration cost. Dornier and Dufay (2013) modeled coevolutionary dynamics of CMS and restorer alleles with a cost under selfing, based on computer simulations. These studies successfully revealed a relationship between both CMS-restorer coevolution and selfing, although they considered selfing only as a fixed parameter. In reality, however, selfing itself can be an evolutionary trait. Indeed, apart from CMS studies, the evolution of selfing has been investigated both empirically and theoretically. Goodwillie et al. (2005) reviewed the history and background of studies surrounding this issue and summarized the theoretical and empirical achievements to date. More recently, Sicard and Lenhard (2011) reviewed the available empirical research on selfing syndrome, in which they discussed a relationship between the two factors that influence the selfing evolution, i.e., ecological and genetic factors. The ecological factors consist of pollen discounting and pollen limitation, which quantitatively affect individual reproductive success. (As described above, those are also important in the evolution of gynodioecy). On the other hand, genetic factors involve inbreeding depression and a "50% automatic advantage of selfing". When a rare mutant with perfect selfing invades a population with outcrossing only, the individual automatically enjoys a 50% advantage of gene transmission because its pollen not only fertilizes the ovules of the resident individuals, but also monopolizes its own ovules (Fisher, 1941, Porcher & Lande, 2005b). Lloyd (1979) theoretically investigated selfing evolution with both inbreeding depression and this automatic advantage and showed that if the loss of seed success by inbreeding depression is smaller than 0.5, selfing can evolve.

Despite the understanding of the importance of selfing evolution in plant reproduction, CMS evolution has not been studied alongside it theoretically. The purpose of the present study is to reveal the effect of the evolution of selfing rate on the coevolution of CMS and nuclear restorer. In this paper, we hypothesize that selfing evolution can suppress the evolution of CMS. For fertilization of ovules, CMS females require hermaphroditic individuals as suppliers of pollen. In the presence of pollen discounting and pollen limitation, selfing reduces the density of exported pollen, by which the evolution of CMS might be suppressed. In order to investigate this process, we theoretically analyze the coevolution of three traits: CMS, nuclear restorer, and selfing rate.

MATHEMATICAL MODEL

In our model, we assume a haploid organism with two nuclear loci, which determine a restoration ability of cytoplasmic male sterility and a selfing rate. Theoretical studies of gynodioecy have traditionally focused on diploid model, although studies of pathogen-plant interaction sometime considered haploid plants (Parker, 1994, Agrawal & Lively, 2002) , which has been accepted as an appropriate approximation. In this study, we also assume haploidy for a simplicity of analysis. The restoration is considered to be controlled by a major gene that involves non-restorer and restorer alleles, genotypes of which are denoted by m and M, respectively. On the other hand, the selfing rate is a quantitative trait that is determined by many genes on quantitative loci with additive effects, which can evolve gradually. In order to analyze evolutionary dynamics of this selfing rate, we assume two genotypes, i.e., a resident selfing allele and a mutant selfing allele, between which the sefing rate is slightly different from each other. The resident and mutant genotypes are denoted by s and s', which also represent their selfing rates. In addition to two nuclear genes, the organism includes a cytoplasmic gene that causes male sterility, which is mutant mitochondria. The genotypes of non-CMS and CMS cytoplasm are defined as n and c, respectively. According to the alternative states on 2 nuclear genes and 1 cytoplasmic gene, there are 8 possible cyto-genotypes, i.e., ms/n, Ms/n, ms/c, Ms/c, ms'/n, Ms'/n, ms'/c, and Ms'/c, genotypic frequencies of which are denoted by X_{mn}, X_{Mn}, X_{mc}, X_{Mc}, X'_{mn}, X'_{Mn}, X'_{mc} and X'_{Mc}, respectively. Primes on the frequencies represent genotypes of mutant with respect to selfing. We assume that there is a linkage between two nuclear loci with a recombination rate r, although it does not influence equilibria and their stabilities.

We assume that male sterility is accompanied by a female advantage, promoting ovule production with a relative advantage k (so that the ovule number becomes $1 + k$), which is achieved only in genotypes ms/c and ms'/c with the CMS and non-restorer allele. It should be noted that our definition of female advantage is different from that of Dornier and Dufay (2013) who analysed an analogous system. In their analysis, female advantage was denoted as a function of selfing rate and inbreeding depression (they expressed it as $k\ w_s/(1 - s\ \delta)$ in a case without the pollen limitation, where w_s represented a negative effect of CMS on ovule production), which represents a relative advantage for inbreeding success. On the contrary to this, we denote female advantage, k, excluding those factors (our $1 + k$ corresponds with $k\ w_s$ in Dornier and Dufay), which we adopt for a convenience in the analysis of selfing evolution.

In this study, we focus on the effects of the selfing rate on coevolution of nuclear restorer and CMS. Selfing influences reproductive success at both the individual and population levels. The first factor is inbreeding depression, which is denoted by a constant δ (i.e., inbreeding success is $1 - \delta$). It should be noted that in reality, inbreeding depression can be a function of selfing rate because selfing tends to sweep out deleterious alleles from the population through strong negative selection on the homozygote of those alleles (Charlesworth et al., 1991, Lande & Schemske, 1985), although we assume a constant inbreeding depression for the simplicity of our analysis. Furthermore, autogamous selfing can reduce the amount of exported pollen if there is a trade-off between pollen number used for self-pollination and outcrossing pollination, i.e., pollen discounting. We denote pollen discounting as a reduction in the number of pollen that an individual releases, which is a function of its selfing rate s as $D_p(s) = 1 - [b + (a - b)s^c]s$, following a formulation by a previous study (Johnston, 1998). In this definition, the negative effect of selfing is expressed as $[b + (a - b)s^c]s$, where a $(0 \leq a \leq 1)$ represents reductions of exported pollen when $s = 1$, b determines the concaveness of the functional form (concave and convex with $a > b$ and $a < b$, respectively), and c (> 0) controls the magnitude of curvature. In addition, $D_p(s)$ is a monotonically decreasing function when $b < a\ (1 + c)/c$. At the population level, the average density of exported pollen can decline with the increase of selfing rate via pollen discounting, and also with the reduction of hermaphrodites as pollen suppliers. The reduction in the density of exported pollen can negatively influence ovule fertilization through pollen limitation. The efficiency of ovule fertilization is defined as an increasing function of the average density of exported pollen P_{EX}, a formulation of which is assumed as $L_p(P_{EX}) = \beta P_{EX} / (\alpha + P_{EX})$. Based on these assumptions, the success of inbreeding and outbreeding are generally weighted by the coefficients $1 - \delta$ and β, respectively. For simplicity, we replace $(1 - \delta) / \beta$ by η. Since $1 - \delta$ is the relative success of inbreeding and β is the maximum fertilization efficiency in outbreeding, η represents the relative advantage of selfing to outbreeding. It should be noted that for outbreeding, the success of exported pollen is determined through pollen competition for ovules, an effect which we incorporate in the model.

We consider that the nuclear restorer is accompanied by costs. Various types of expressions are possible for this disadvantage of restoration (Bailey et al., 2003, Dufay et al., 2007). In the present study, we consider two types of negative effect of the restorer allele, in which the restorer allele may reduce either male function (pollen production) or individual performance (relative survivorship of individual) from 1 to $1 - \mu$ ($\mu \leq 1$) in a relative value, which are hereafter referred to as cost types 1 and 2, respectively. Those costs incur in individuals with a restorer allele independently of their cytotypes, which is the so-called "constitutive cost" in the definition by Dufay et al. (2007). Remarkably, it was reported that in *Lobelia siphilitica*, nuclear restore decreased pollen viability even when it did not affect sex determination due to a mismatch of specificity to CMS (Bailey, 2002), which may partly correspond with our cost type 1. We could also consider alternative types of restoration costs that decrease female success only, although dynamic equations are difficult to solve explicitly in this case. Therefore, we exclude this type of cost in the present analysis.

Under cost type 1, the male functions of both CMS and non-CMS individuals with the restorer allele are lower than that of an individual without it, and therefore the average density of exported pollen is affected by the restoration cost, a relative value, $P_{EX} = \{X_{mn} + (1 - \mu)(X_{Mn} + X_{Mc})\}D_p(s) +$

$\{X'_{mn} + (1-\mu)(X'_{Mn} + X'_{Mc})\}D_p(s')$. On the other hand, under cost type 2, the frequencies of both CMS and non-CMS individuals with the restorer allele decline immediately before a measurement of their genotypic frequencies. In this case, the average density of exported pollen is $P_{EX} = (X_{mn} + X_{Mn} + X_{Mc})D_p(s) + (X'_{mn} + X'_{Mn} + X'_{Mc})D_p(s')$. This expression does not include the restoration cost μ because the costs have already affected the genotypic frequencies before the census of frequency. The densities of pollen influence outbreeding success through the fertilization efficiency of ovules due to pollen limitation, and the competition among pollen for ovules.

Based on those assumptions, we formulate the dynamics of genotypic frequencies by combining the reproductive outcomes of selfing and outbreeding. Here, we show frequency dynamics of strains with resident selfing rate under cost type 1 in the absence of mutant strains as simple examples. For simplicity of description, we refer to X_{mn}, X_{Mn}, X_{mc}, and X_{Mc} by w, x, y, z, with which dynamics are

$$w_{t+1} = \left[(1-\delta)sw_t + \frac{\beta P_{EX}}{\alpha + P_{EX}} D_p(s)(1-s)\left\{\frac{w_t}{P_{EX}}\left(w_t + \frac{1}{2}x_t\right) + (1-\mu)\frac{x_t + z_t}{P_{EX}}\frac{1}{2}w_t\right\}\right]\frac{1}{W}\ , \tag{1a}$$

$$x_{t+1} = \left[(1-\delta)sx_t + \frac{\beta P_{EX}}{\alpha + P_{EX}} D_p(s)(1-s)\left\{\frac{w_t}{P_{EX}}\frac{1}{2}x_t + (1-\mu)\frac{x_t + z_t}{P_{EX}}\left(\frac{1}{2}w_t + x_t\right)\right\}\right]\frac{1}{W}\ , \tag{1b}$$

$$y_{t+1} = \frac{\beta P_{EX}}{\alpha + P_{EX}} D_p(s)(1-s)\left\{\frac{w_t}{P_{EX}}\left((1+k)y_t + \frac{1}{2}z_t\right) + (1-\mu)\frac{x_t + z_t}{P_{EX}}(1+k)\frac{1}{2}y_t\right\}\frac{1}{W}\ , \tag{1c}$$

$$z_{t+1} = \left[(1-\delta)sz_t + \frac{\beta P_{EX}}{\alpha + P_{EX}} D_p(s)(1-s)\left\{\frac{w_t}{P_{EX}}\frac{1}{2}z_t + (1-\mu)\frac{x_t + z_t}{P_{EX}}\left((1+k)\frac{1}{2}y_t + z_t\right)\right\}\right]\frac{1}{W}\ , \tag{1d}$$

where W represents the average fitness. Variables, parameters and functions that are used in the present model are summarized in Table 1. Full dynamics of the system are shown in the Appendix A.

Equilibrium mating modes under a fixed selfing rate

First, we investigate the dynamics in a population with a homogeneous selfing rate without a mutant selfing rate, i.e., $(X'_{mn}, X'_{Mn}, X'_{mc}, X'_{Mc}) = (0, 0, 0, 0)$. Under both cost types 1 and 2, there are six types of equilibria, two out of which are equilibrium states with a single genotype only. One equilibrium is $(X_{mn}, X_{Mn}, X_{mc}, X_{Mc}) = (1, 0, 0, 0)$ that comprises a genotype with neither restorer nor CMS, which is always feasible, but stable only if $\{k(1-s)-s\eta\}D_p(s) < s\alpha\eta$. Another solution is (0, 0, 0, 1) with a fixation of both restorer allele and CMS cytotype. It should be remarked that this solution is a subset of an equilibrium with two genotypes $(0, X_{Mn}, 0, X_{Mc})$. The systems also generally have three types of equilibria with two genotypes, and a unique solution with a coexistence of four genotypes. Properties of those equilibria with multiple genotypes depend on cost types.

For cost type 1, genotypic frequencies are

$$(X_{mn}, X_{Mn}, X_{mc}, X_{Mc}) = (0, X_{Mn}, 0, X_{Mc}), \tag{2a}$$

$$(X_{mn}, X_{Mn}, X_{mc}, X_{Mc}) = \left(0,\ 0,\ 1-\frac{2s\alpha\eta+(1+k)(1-s)(1-\mu)D_p(s)}{2\{k(1-s)-s\eta\}(1-\mu)}, \frac{2s\alpha\eta+(1+k)(1-s)(1-\mu)D_p(s)}{2\{k(1-s)-s\eta\}(1-\mu)}\right), \tag{2b}$$

$$(X_{mn}, X_{Mn}, X_{mc}, X_{Mc}) = \left(\frac{s\alpha\eta}{\{k(1-s)-s\eta\}D_p(s)},\ 0,\ 1-\frac{s\alpha\eta}{\{k(1-s)-s\eta\}D_p(s)},\ 0\right), \tag{2c}$$

$$(X_{mn}, X_{Mn}, X_{mc}, X_{Mc}) =$$

$$\left(\frac{1+k}{k}\ \frac{s\alpha\eta-\{k(1-s)-s\eta\}(1-\mu)D_p(s)}{\{k(1-s)-s\eta\}\mu D_p(s)}, \frac{1}{k\mu}\left((1+k)(1-\mu)-\frac{s\alpha\eta\{1+k(1-\mu)\}}{\{k(1-s)-s\eta\}D_p(s)}\right),\right.$$

$$\left.\frac{1}{k}\left(-1+\ \frac{s\alpha\eta}{\{k(1-s)-s\eta\}(1-\mu)D_p(s)}\right),\ \frac{1}{k}\left(1+k-\ \frac{s\alpha\eta\{1+k(1-\mu)\}}{\{k(1-s)-s\eta\}(1-\mu)D_p(s)}\right)\right). \tag{2d}$$

Equilibrium (2a) is a line rather than a point, which also includes (0, 0, 0, 1). The feasibility and stability conditions of equilibria are summarized in Table 2. The stability condition of the last equilibrium is too complex to be derived analytically, so are examined numerically based on the eigenvalues of the Jacobian matrix of the dynamics. Examples of parameter dependence of those conditions are illustrated in Figure 1 under the parameter set given in Table 1. (We also supplementally check the robustness of this trend with varying parameters (see below)).

On the other hand, those for the cost type 2 are

$$(X_{mn}, X_{Mn}, X_{mc}, X_{Mc}) = (0, X_{Mn}, 0, X_{Mc}), \tag{3a}$$

$$(X_{mn}, X_{Mn}, X_{mc}, X_{Mc}) =$$

$$\left(0,\ 0,\ 1-\frac{(1-\mu)\{2s\alpha\eta+(1+k)(1-s)D_p(s)\}}{[(1-s)\{k(2-\mu)+\mu\}-2s\eta(1-\mu)]D_p(s)},\frac{(1-\mu)\{2s\alpha\eta+(1+k)(1-s)D_p(s)\}}{[(1-s)\{k(2-\mu)+\mu\}-2s\eta(1-\mu)]D_p(s)}\right), \tag{3b}$$

$$(X_{mn}, X_{Mn}, X_{mc}, X_{Mc}) = \left(\frac{s\alpha\eta}{\{k(1-s)-s\eta\}D_p(s)},\ 0,\ 1-\frac{s\alpha\eta}{\{k(1-s)-s\eta\}D_p(s)},\ 0\right), \tag{3c}$$

$$(X_{mn}, X_{Mn}, X_{mc}, X_{Mc}) =$$

$$\frac{1}{\{2s\eta(1+k\mu)+k(k-1)(1-s)(1-\mu)\}D_p(s)}\times$$

$$\left(\frac{[2s\alpha\eta(k+\mu)-(1+k)\{k(1-s)-2s\eta\}(1-\mu)D_p(s)][s\alpha\eta(1+k\mu)+\{s\eta(1+k\mu)-k(1-s)(1-\mu)\}D_p(s)]}{s\eta\mu\{(k-1)\alpha+(1+k)D_p(s)\}},\right.$$

$$\frac{-2(s\alpha\eta)^2(1+\mu)(k+\mu)+(1-\mu)\langle s\alpha\eta[k(1-s)\{k(3+\mu)+(1+3\mu)\}-2s\eta\{k(2+\mu)+(1+2\mu)\}]-(1+k)\{k(1-s)-s\eta\}\{k(1-s)-2s\eta\}(1-\mu)D_p(s)\rangle D_p(s)}{s\eta\mu\{(k-1)\alpha+(1+k)D_p(s)\}},$$

$$2[s\alpha\eta(1+k\mu)+\{s\eta(1+k\mu)-k(1-s)(1-\mu)\}D_p(s)],$$

$$\left.-2(1+k)[s\alpha\eta(1+\mu)-\{k(1-s)-s\eta\}(1-\mu)]D_p(s)\right)\ . \tag{3d}$$

The equilibrium Eq. (3a) is a line rather than a point, which includes (0, 0, 0, 1). The feasibility and stability conditions of equilibria are summarized in Table 2. Both feasibility and stability conditions of equilibrium (3d) are too complex to be derived analytically, which are examined numerically. Examples of parameter dependence of those conditions are illustrated in Figure 2.

Both Figs. 1 and 2 indicate that the conditions of equilibrium do not overlap each other, except for equilibria (2a) and (3a) which can be bistable with three other equilibria, (1, 0, 0, 0), Eqs. (2c) or (2d) under cost type 1, and (1, 0, 0, 0), Eqs. (3c) or (3d) under cost type 2, respectively (see regions bounded by broken curves). The bistabilities result from a strong positive frequency-dependent selection between non-restorer allele and non-CMS mitochondria. Equilibria (2a) and (3a) associate with a fixation of restorer allele, where CMS mitochondria is neutral due to a suppression of male-sterility. In this case, the frequency of CMS mitochondria changes only by genetic drift, in which the state is relatively stable. On the other hand, when the frequency of CMS cytotype is comparatively low, an advantage of restoration is small, in which the restoration allele cannot increase due to its accompanying cost. These reciprocal suppressions cause bistability of the two equilibria.

The trends are similar between Figs. 1 and 2, although there are clear differences. In Fig. 1, a hermaphrodite population with a fixation of restorer allele (i.e., $(0, X_{Mn}, 0, X_{Mc})$) tends to occur in relatively wide parameter regions in comparison to Fig. 2. Contrary to this, regions of cytoplasmic gynodioecy without restorer (i.e., $(X_{mn}, 0, X_{mc}, 0)$) become wider in Fig. 2. These differences may result from the influence of a restoration cost on the frequency of the restorer allele. In cost type 1, the restoration cost decreases the restorer alleles in the pollen pool only, but not in the ovule pool, which may mildly suppress restorer evolution. On the other hand, with regards to cost type 2, the restoration cost decreases restoration alleles totally in the entire population, which significantly suppresses the prevalence of the restoration allele. It should be remarked that simple comparisons between two cost cases might be inadequate because the relative effect of pollen limitation is different between those, owing to a difference of census timing of genotypic frequencies (before and after suffering restoration cost in cost types 1 and 2, respectively). However, such comparisons could provide useful information to understand some evolutionary trends.

In order to study transient dynamics, we conduct simulations for some example cases, which are illustrated in Figure 3. Figs. 3(a)-(c) represent results in the bistable cases. In the equilibrium (2a) on the X_{Mn}-X_{Mc} axis, CMS mitochondria is neutral owing to restorer fixation, where genetic drift causes the fluctuation of its frequency. Importantly, when the CMS frequency (i.e., X_{Mc}) falls below a threshold, the state becomes unstable, causing an increment in the non-restorer allele. Figure 3(d) illustrates that if the equilibrium (2a) is a unique solution, trajectories starting from an unstable region on the X_{Mn}-X_{Mc} axis finally return to the stable region on the same axis with the disappearance of the non-restorer allele.

Accordingly, a combination of genetic drift on mitochondria and the mutational occurrence of non-restorer allele may result in intermittent repeating cycles.

Selfing evolution from perfect outbreeding and perfect selfing

We considered a constant selfing rate in the above analysis, although in reality selfing rate can evolve. This evolution of selfing is analyzed by examining the invasibility of individuals with a mutant selfing rate into a population with a resident selfing rate. We assume that the population always reaches an equilibrium state of restorer and CMS for the resident selfing rate. This assumption may be reasonable because the selfing rate is a quantitative trait which changes more slowly and continuously than allelic dynamics of restorer and CMS. Under bistability of two equilibria, we consider that the system eventually converges to an equilibrium other than Eqs. (2a) and (3a) because those equilibria can be unstable due to genetic drift (see above). In addition to this, when equilibrium (2a) or (3a) is a unique stable solution, we assume that (0, 0, 0, 1) is the realized equilibrium because a fixation of CMS mitochondria can persist for a relatively long time until an emergence of non-CMS mitochondria.

First, we analytically investigate the dynamics at the boundary selfing rates, i.e., perfect outbreeding (s = 0) and perfect selfing (s = 1), by analyzing eigenvalues of the Jacobian matrix of the system with resident and mutant selfing rates. According to Eqs. (2) and (3), at perfect outbreeding with s = 0, three types of equilibria occur conditionally in both cost types, i.e., (0, 0, X_{mx}, X_{Mc}), (0, 0, 0, 1) and (1, 0, 0, 0) (see also Figs. 1 and 2). In those equilibria, the perfect outbreeding can be either stable or unstable, depending on conditions. For cost type 1, the instability conditions of perfect outbreeding are

$$2\eta\left(1+\frac{2k\alpha}{(1-\mu)(1+k)}\right)-k(1+b)>0 \qquad \text{for} \qquad (0, 0, X_{mc}, X_{Mc})\,, \tag{4a}$$

$$2\eta\left(1+\frac{\alpha}{1-\mu}\right)-(1+b)>0 \qquad \text{for} \qquad (0, 0, 0, 1)\,, \tag{4b}$$

$$2\eta(1+\alpha)-(1+b)>0 \qquad \text{for} \qquad (1, 0, 0, 0)\,. \tag{4c}$$

On the other hand, those for cost type 2 are

$$2\eta\left(1-\mu+\frac{\alpha\{2k+(1-k)\mu\}}{1+k}\right)-(k+\mu)(1+b)>0 \quad \text{for} \quad (0, 0, X_{mc}, X_{Mc})\,, \tag{5a}$$

$$2\eta(1+\alpha)-(1+b)>0 \quad \text{for} \quad (0, 0, 0, 1)\,, \tag{5b}$$

$$2\eta(1+\alpha)-(1+b)>0 \quad \text{for} \quad (1, 0, 0, 0)\,. \tag{5c}$$

Under these conditions, selfing can evolve from perfect outbreeding. These conditions tend to be satisfied by larger α and η (= (1 - δ) / β), and smaller b, which promotes the evolution of selfing. In addition, from Eqs. (4a) and (5a), we can prove that an increment of k suppresses the evolution under the feasibility and stability conditions of those equilibria. Significantly, an increment of μ promotes selfing evolution in Eqs. (4a) and (4b) but suppresses it in Eq. (5a). This indicates that in equilibria with a fixation of restorer allele, restoration costs conversely affect the selfing evolution from perfect outbreeding depending on cost types. Mechanisms of those parameter dependencies are discussed below (see Discussion).

We also analyze selfing evolution from perfect selfing (s = 1). It can be analytically shown that with s = 1, the original hermaphrodite state, (1, 0, 0, 0), is a unique stable equilibrium in both cost types due to an exclusion of (0, X_{Mn}, 0, X_{Mc}) from consideration under bistability (see also Figs. 1 and 2). At equilibrium, perfect selfing can be stable when

$$2\eta\left(\frac{\alpha}{1-a}+1\right)>1\ , \tag{6}$$

regardless of cost type. This indicates that under both cost types 1 and 2, perfect selfing tends to persist when α, a or η (= (1 - δ) / β) is large (see Discussion). The effects of parameters on instabilities of boundary selfing rates are summerized in Table 3.

Evolution of intermediate selfing rate

Next, we examine the evolution of an intermediate level of selfing rate. The Jacobian matrix of system with $0 < s < 1$ is very complex. In addition to this, equilibrium mating mode discontinuously change with varying selfing rate. These properties mean that analytical derivations of the maximum eigenvalue and its derivative are difficult, therefore, we analyze evolutionary dynamics numerically (see Appendix B). In Figures 1 and 2, solid circles represent selfing rates that are simultaneously convergently and evolutionary stable, whereas open circles indicate such that are convergently unstable. In each panel, the selfing rate evolves along a horizontal direction under a given k value. In the examined case, all convergently stable solutions satisfy evolutionary stability conditions at least under the given conditions. These figures indicate that there can be multiple convergently and evolutionarily stable solutions in the evolution of selfing, and that intermediate selfing rates can be evolutionarily realized depending on parameters. These figures imply that the evolution of selfing rate realizes multiple equilibria, which associate with various types of mating modes.

According to the numerical analysis, all solutions that are indicated by solid circles in Figs. 1 and 2 are satisfied both convergent and evolutionary stability conditions. In order to examine the evolutionary dynamics of selfing in more detail, we conducted supplemental analysis (see Appendix B), and illustrate a PIP (pairwise invasibility plot) that represent the invasibilities of mutant strategies into populations with resident strategies (Geritz et al., 1998). Supplementary figures 1 and 2 show PIP for $k = 1$ cases of Figs. 1 and 2, respectively, by which we can reconfirm evolutionary stabilities of the solid circles graphically.

Figures 1 and 2 focus on effects of cost of restorer (μ) and inbreeding depression (δ) on evolution of mating mode and selfing rate. We also examine dependencies of evolution on parameters of pollen limitation (α and β) and pollen discounting (a and b), which are illustrated in Supplementary figures 3-10 (those trends are discussed below). It is remarkable that all results indicate that once selfing rate evolves toward some level, it can prevent CMS mitochondria from fixation. If selfing rate evolves toward $s = 1$, both restorer and CMS are excluded from the population (i.e., (1, 0, 0, 0)), which represents a negative correlation between selfing, and CMS and restorer in their coevolution. It should be noted that that with a parameter set of panels (a) in Supplementary Figs. (7)-(10), a pollen discounting function $D_p(s)$ is not a monotonically decreasing function within $0 \leq s \leq 1$, which is locally minimized around $s = 0.69444$. However, those figures suggest that a small deviation from monotonically decreasing manner in pollen discounting does not affect trends significantly.

DISCUSSION

Multi-stability in the analyzed system

Throughout the analyses, we clarify the effect of selfing on the coevolution of nuclear restorer and CMS cytoplasm. First, we demonstrate the bistability of equilibria under a fixed selfing rate, which was first proposed by Charlesworth (1981) but had not been studied in detail. In the present study, we analytically clarify the conditions for bistability of mating modes in relation to selfing rate. The bistability results from a positive frequency-dependent selection between non-restorer allele and non-CMS mitochondria. The possibility of bistability suggests that if local populations are founded by small groups with various genotypic compositions, steady states might differ among those local populations in a single species. Remarkably, the present analysis shows that one equilibrium in bistability is always the hermaphroditic population with a fixation of restorer allele (i.e., $(0, X_{Mn}, 0, X_{Mc})$). In this case, the frequency of CMS mitochondria is neutral on an X_{Mn}-X_{Mc} axis, which can lead the equilibrium to a region of instability due to genetic drift. Thus, this state ultimately becomes unstable and subsequently converges to an alternative equilibrium. Although the hermaphroditic population with a fixation of restorer could result from founder effects in colonization or stochasticity in dynamics, it may not persist for a long period.

Subsequently, evolution of selfing are included in the model, by which we investigate coevolutionary process of three traits, i.e., selfing rate, nuclear restorer and CMS. According to the analysis, multiple selfing rates (including $s = 0$ and 1) can be stable simultaneously under given parameter values and conditions (Figs. 1 and 2). As described above, bistability is possible even with the fixed selfing rate. When we take into account the evolution of selfing, a greater number of diverging states can be possible due to the combination of multi-stabilities of both the CMS-restorer interaction and the realized selfing rate.

It is known that gynodioecious species often show extremely wide variation in female frequencies among populations (Lloyd, 1976, Frank, 1989, Webb, 1999). In addition to this, selfing rates are known to vary among populations of gynodioecious species (Dornier & Dufay, 2013). Diversities that are observed in gynodioecious species may be explained by the property of multi-stability of gynodioecy, which is indicated by the analysis presented in this study. Under the multi-stability of mating systems, stochasticities in dynamics and a founder effect in colonization may cause significant fluctuation or variation in system states, which may result in a variation of selfing rates. Interestingly, female frequencies in nuclear gynodioecy tend to be stable among populations in comparison to nuclear-cytoplasmic gynodioecy (Bailey & Delph, 2007a). Figs.1 and 2 show that nuclear gynodioecy is generally monostable without an alternative equilibrium state, which may be a reason for the relative stability of nuclear gynodioecy.

Driving force for the evolution of selfing from perfect outbreeding

The main driving force of selfing evolution may be due to the reproductive assurance of hermaphrodite individuals under pollen limitation. In a CMS-prevailing population, the average density of exported pollen is low because female individuals with CMS don't export pollen at all. In those cases, hermaphroditic individuals evolve higher selfing rates to ensure their ovule fertilization. This selfing evolution further intensifies the lack of exported pollen in the population under pollen discounting, consequently suppressing the evolution of CMS that requires pollen, in other words, the enclosure of pollen by hermaphroditic individuals via selfing subdues CMS cytoplasm.

This scenario is supported by an examination of the effects of pollen limitation on selfing evolution. Under pollen limitation, the fertilization of outbred ovules increases with the average density of exported pollen, In the presented model, the function of pollen limitation is determined by two parameters, α and β, which represent an insensitivity of fertilization improvement to pollen density and a maximum level of fertilization respectively, where larger α and smaller β indicate more intensive pollen limitation. Our analysis shows that selfing can evolve from perfect outbreeding under larger α and smaller β (see Eqs. (4) and (5)). This is also supported by supplementary analysis, showing that selfing rate tends to evolve toward higher levels under larger α and smaller β (Supplementary Figs. 3-6). Namely, strong pollen limitation results in higher selfing rates, which is consistent when considering selfing evolution as a reproductive assurance.

We also examine the effects of pollen discounting on selfing evolution. Under intensive pollen discounting, an increase in an individual's selfing rate results in a significant reduction in pollen which is exported by the individual. In our model, pollen discounting is determined by two parameters, a and b. In the pollen discounting function, a represents the reduction of exported pollen at perfect selfing ($s = 1$), whereas b determines the concaveness of the function, i.e., a large b causes a steep reduction of exported pollen at a small selfing rate. Accordingly, it is expected that both large a and b intensify pollen discounting, resulting in similar effects on selfing evolution. However, this should be considered more carefully because the effects of these two parameters on pollen discounting are not straightforward. Here, we focus on a population with a low selfing rate, where outbreeding is dominant (a case with a higher selfing rate is discussed below, where the results are completely different). Under intense pollen discounting, an individual with selfing exports a small amount of pollen, which spoils an individual's ability in competition among pollen for ovules. This disadvantage is significant in the outbreeding-dominant population, which suppresses selfing evolution at low selfing rates via a negative feedback. Importantly, within a range of low selfing rates, the sensitivity of the pollen discounting function to the selfing rate is mainly governed by the parameter b (but not by a), therefore, smaller b is expected to promote selfing evolution. Indeed, our analysis shows that selfing evolution from perfect outbreeding is promoted by smaller b, but is independent of a (see Eqs. (4) and (5)). In contrast, lager b suppresses selfing evolution via a negative feedback between selfing and pollen discounting. The effect of b at low selfing rates can be also confirmed in Supplementary Figs. 7-10.

According to the present analysis, when the advantage of CMS in female is high (larger k), selfing evolution from perfect outbreeding tends to be suppressed in the population of nuclear gynodioecy, $(0, 0, X_{mc}, X_{Mc})$ (see Eqs. (4a) and (5a), and Figs. 1 and 2). When females with CMS produce more ovules, selfing reduces the opportunity to fertilize many ovules through outbreeding (i.e., higher male success in a female-biased population), a disadvantage by which may suppress selfing evolution. It should be noted that this mechanism is effective only when nuclear genes have some transition pathways from female to hermaphroditic individuals, i.e. the existence of some levels of restorer. (Otherwise, after fertilization with ovules of female individuals, the selfing modifier loses any opportunities to be expressed and to be selected). On the other hand, in a hermaphroditic population ((0, 0, 0, 1) and (1, 0, 0, 0)), the advantage of CMS in females does not affect selfing evolution from perfect outbreeding (see Eqs. (4b, c) and (5b, c), and Figs. 1 and 2). Such a population comprises no females regardless of an existence of CMS mitochondria, in which an advantage of CMS in females is not effective to selfing evolution.

We find that in nuclear gynodioecy, (0, 0, X_{mc}, X_{Mc}) being stable with $k > 0$, the effect of the restoration cost (μ) on selfing evolution from perfect outbreeding depends on the cost type. The effect is promotional in a cost reducing male function (Eq. (4a)), but suppressive in a cost reducing individual performance (Eq. (5a): its left-hand side term is negative and positive at small and large μ, respectively, when its sign changes within $0 \leq \mu \leq 1$). In a population with the cost reducing male function, the larger cost significantly decreases individual pollen production, causing lower average density of exported pollen. In this case, ovules are unlikely to be fertilized by outbreeding under pollen limitation, by which selfing becomes more preferable via intensified reproductive assurance. On the other hand, the cost reducing individual performance does not influence the average density of exported pollen in the population (see above). Instead, the cost totally decreases hermaphroditic individuals that carry a restorer allele, which relatively increases the frequency of CMS females, realizing in a female-biased sex ratio. In this case, exported pollen can achieve a high fertilization success via outbreeding with many females, by which the larger restorer cost suppresses selfing evolution (importantly, those offspring can also be hermaphroditic due to the inheritance of the restorer gene in nuclear gynodioecy). Those mechanisms may result in the opposite dependencies of selfing evolution on the restoration cost between nuclear gynodioecy with different cost types. In the presented analysis, we do not consider alternative types of restoration costs that decrease female success only. In reality, however, it was reported that hermaphrodites carrying nuclear restorer genes had lower seed quantity in *Plantago lanceolata* (de Haan et al., 1997). This type of cost does not influence the average density of exported pollen, but reduce a number of ovules of restored hermaphrodites, which may be also suppressive for selfing evolution.

Evolution of higher levels of selfing

According to the present analysis, intermediate levels of selfing can be achieved evolutionarily in a gynodioecious system. The evolution of intermediate levels of selfing has been a subject of theoretical discussion because it cannot be represented simply (see a review by Goodwillie et al. (2005)). For the stability of intermediate selfing rates, a factor with negative frequency dependence on selfing rate is required. Johnston (1998) indicated that the existence of pollen discounting can result in intermediate levels of selfing that are both convergently and evolutionarily stable, a mechanism which could be effective also in the presented model. Remarkably, the author derived a unique stable solution for an intermediate level of selfing under a given condition, although our model shows the possibility of multiple solutions at intermediate levels (see, for example, Fig. 1(i) with $k = 1.3$). This is because CMS-restorer status can change depending on the selfing rate. In Fig. 1(i), one intermediate level of selfing involves a nuclear gynodioecy with a CMS fixation, whereas another solution is accompanied by a cytoplasmic-nuclear gynodioecy that is potentially bistable with a hermaphrodite. The bistability of intermediate levels of selfing is a characteristic property of the coevolution of CMS, restorer and selfing rate.

In the above discussion of selfing evolution from perfect outbreeding, we explain that selfing evolution is suppressed by intense pollen discounting with large b (the concaveness of the functional form), independently of the value of a (reductions of exported pollen when $s = 1$). The trend varies in a population with high selfing rates. In the selfing-dominant population, intense pollen discounting significantly reduces the average density of exported pollen, in which selfing is favored as a reproductive assurance under pollen limitation. In short, under high selfing rates, strong pollen discounting tends to promote selfing evolution. Importantly, at high selfing rates, a parameter a mainly governs the sensitivity of the pollen discounting function to the selfing rate, by which selfing evolution is expected to be promoted by larger a. Such a trend can be confirmed in Supplementary Figs. 7-10 (it should be noted that stable selfing solutions with intermediate values also exist above the plotted range in those figures). Consequently, the effect of pollen discounting on selfing evolution at high selfing rate is opposite to that at low selfing rate, which tends to be controlled by different parameters, a and b, respectively.

It should be noted that intense pollen discounting can result in a positive feedback in selfing evolution in response to CMS prevalence. When CMS evolves and dominates in the population, a scarcity of hermaphrodites that are suppliers of exported pollen intensifies pollen limitation in outbreeding, by which selfing could be favored to ensure reproductive success in hermaphroditic individuals. If the pollen discounting is strong, the increment of selfing rate tends to reduce the average density of exported pollen significantly, which enhances the importance of reproductive assurance. These processes accelerate the evolution of higher selfing rates with a positive feedback between pollen limitation and reproductive assurance through pollen discounting, which gradually suppresses CMS females that require pollen supply from hermaphrodites. The cascade is triggered by CMS evolution and eventually suppress CMS.

The presented analysis also shows that perfect selfing ($s = 1$) can be stable under low inbreeding depression (small δ), strong pollen discounting (large a), and intensive pollen limitation (large α and small β) (see Eq. (6)). Namely, when both pollen limitation and pollen discounting are strong, perfect selfing tends to be stable (see also Supplementary Figs. 3-10). This can be explained by individuals with perfect selfing ($s = 1$) exporting little pollen in the presence of pollen discounting, by which a lower selfing mutant finds it difficult to outbreed successfully under intense pollen limitation, resulting in a failure of its invasion.

Influence of selfing evolution on gynodioecy

Our analysis shows that the evolution of selfing significantly influences the CMS-restorer interaction. If the selfing rate reaches an intermediate level, nuclear-cytoplasmic gynodioecy and cytoplasmic gynodioecy can be achieved (Figs. 1(e), (f), (i), and 2(a), (e), (f), (i)). Furthermore, if selfing reaches a perfect level ($s = 1$), a hermaphrodite population occurs with neither CMS nor restorer. Namely, when selfing rate evolves toward a substantial level, CMS and restorer are likely to be excluded from the population. This trend is inconsistent with the results of Dornier and Dufay (2013), which illustrated that evolution of nuclear gynodioecy was promoted under higher selfing rates (in Dornier and Dufay, Fig. 3). This may be explained by the absence of pollen limitation in their examined cases.

When selfing cannot evolve or stay at very low level ($s \approx 0$), either CMS or restorer allele would be fixed in the population with $k > 0$, which may imply that the failure of selfing evolution intensifies an arms race between CMS and restoration. It should be remarked that with a sufficiently large k, there are also some advantages for non-restore allele. When CMS persists under large k, female individuals with CMS achieve a high reproductive success. In this case, non-restorer allele can increase by hitchhiking on this female advantage, which is a reason that both restorer and non-restorer alleles coexist with a fixation of CMS cytotype under $k > 1$. On the other hand, the evolution of intermediate levels of the selfing rate ($s > 0$) promotes the coexistence of non-CMS and CMS cytotypes, and non-restorer and restorer alleles. If the selfing rate reaches a very high level ($s \approx 1$), both CMS and restorer allele are eliminated from the population, implying that intense selfing suppresses CMS evolution.

Lahiani et al. (2015) studied reproductive assurance in nuclear-cytoplasmic gynodioecious species, *Silene nutans* (Caryophyllaceae), which categorized plant habitats into female-biased or hermaphrodite-biased patches. The authors showed that female-biased patches were characterized by more fruit set and higher selfing rate than hermaphrodite-biased patches, which suggested a correlation between female advantage (k) and selfing rate (s). The analysis that is presented here predicts a positive correlation between female advantage (k) and selfing rate (s) in nuclear-cytoplasmic gynodioecy (see

Figs.1(e) and (i)). Although a relationship between those values and female ratio is not simple in our analysis (see Eqs. (2d) and (3d)), the observed positive correlation between female advantage and selfing rate is consistent with results of our models, which can be explained by evolution of selfing rate under a given parameter k in the gynodioecious plant.

Implications of observed gynodioecy

Our analysis successfully indicates an evolutionary relationship between gynodioecy and selfing, although it is inconsistent to some observations of selfing in gynodioecy. Dornier and Dufay (2013) reviewed selfing in gynodioecious plants, which indicated that some levels of selfing were observed in nuclear gynodioecy. In our results, nuclear gynodioecy occurs in a region with high female advantage in CMS (large k) and low selfing rate (small s), where stable selfing rates tend to be 0 or small (see Figs. 1 and 2, and Supplementary figures). This inconsistency may imply that additional factors are needed to understand the coevolution of gynodioecy and selfing. In the presented study, we focus on dynamics of genotypic frequencies, ignoring population dynamics that may influence mating processes. In addition, we considered pollen discounting is a function of average density of pollen only, although it might be also influenced by an ovule density typically in animal pollination systems via an efficiency of pollinator attraction. Inclusions of such factors may alternate trends of selfing evolution.

There is also another inconsistency in the present model. It is known that cytoplasmic gynodioecy without restoration is very rare in plants (Burt & Trivers, 2009), although it can be achieved in our model. When the cost of restoration is high (large μ), cytoplasmic gynodioecy without restorer (i.e., (X_{mn}, 0, X_{mc}, 0)) is possible within regions of intermediate levels of selfing, which can be an equilibrium of selfing evolution (see Figs. 1(f), and 2(e), (f), (i)). This trend is less significant in the case that restorer cost reduces male function (Fig. 1), especially when the relative advantage of selfing (η) is small (compare between Figs. 1(f) and (i)). In such a case, instead, nuclear-cytoplasmic gynodioecy is possible (Fig. 1(i)), which is widely observed in natural populations (Delph et al., 2007). This may suggest that in plant species the restorer cost tends to affect male function, and that a relative advantage of inbreeding to outbreeding ($\eta = (1 - \delta) / \beta$) may be relatively small. It was reported that hermaphrodites carrying nuclear restorer genes had lower pollen viability in *Lobelia siphilitica* (Bailey, 2002), which may suggested that the restorer cost on male function is not rare.

In the present analysis, we combine a major gene model (for CSM and restorer) and an adaptive dynamics model (for selfing rate), by which successfully revealed properties of coevolution of gynodioecy and selfing rate. Selfing is generally expected to influence the evolution of cytoplasmic genetic element (CGE) because it affects the inheritance processes of CGEs. Accordingly, the present analysis provides a basis to study evolution of a wide variety of selfish CGEs. For instance, selfing in plants may corresponds with sib mating in animals, therefore it might be also applicable to inter-genomic conflict in animals with sib mating. Our approach involves a potential to contribute on investigations about properties of various intergenomic conflicts.

ACKNOWLEDGMENTS

We thank Dr. K. Ito and the members of the Centre for Ecological Research for their comments and encouragement. This research was supported financially by JSPS KAKENHI Grant Numbers 15K07219 and 19K06851 to A.Y. This research was partly supported by the International Research Unit of Advanced Future Studies at Kyoto University to A.Y., and partly supported by a JSPS summer fellowship awarded to R.D.B. We also appreciate helpful suggestions and comments of two anonymous reviewers.

REFERENCES

Agrawal, A. & Lively, C. M. 2002. Infection genetics: gene-for-gene versus matching-alleles models and all points in between. *Evolutionary Ecology Research* **4**: 79-90.

Bailey, M. F. 2002. A cost of restoration of male fertility in a gynodioecious species, Lobelia siphilitica. *Evolution* **56**: 2178-2186.

Bailey, M. F. & Delph, L. F. 2007a. A field guide to models of sex-ratio evolution in gynodioecious species. *Oikos* **116**: 1609-1617.

Bailey, M. F. & Delph, L. F. 2007b. Sex-ratio evolution in nuclear-cytoplasmic gynodioecy when restoration is a threshold trait. *Genetics* **176**: 2465-2476.

Bailey, M. F., Delph, L. F. & Lively, C. M. 2003. Modeling gynodioecy: Novel scenarios for maintaining polymorphism. *American Naturalist* **161**: 762-776.

Burt, A. & Trivers, R. 2009. *Genes in conflict: The biology of selfish genetic elements*. Harvard University Press, Harvard.

Charlesworth, B. 1980. The cost of sex in relation to mating system. *Journal of Theoretical Biology* **84**: 655-671.

Charlesworth, B., Morgan, M. T. & Charlesworth, D. 1991. Multilocus models of inbreeding depression with synergistic selection and partial self-fertilization. *Genetical Research* **57**: 177-194.

Charlesworth, D. 1981. A further study of the problem of the maintenance of females in gynodioecious species. *Heredity* **46**: 27-39.

Charlesworth, D. & Ganders, F. R. 1979. Population-genetics of gynodioecy with cytoplasmic-genic male-sterility. *Heredity* **43**: 213-218.

de Haan, A. A., Hundscheid, M. P. J. & vanHinsberg, A. 1997. Effects of CMS types and restorer alleles on plant performance in Plantago lanceolata L.: an indication for cost of restoration. *Journal of Evolutionary Biology* **10**: 803-820.

Delannay, X., Gouyon, P. H. & Valdeyron, G. 1981. Mathematical study of the evolution of gynodioecy with cytoplasmic inheritance under the effect of a nuclear restorer gene. *Genetics* **99**: 169-181.

Delph, L. F., Touzet, P. & Bailey, M. F. 2007. Merging theory and mechanism in studies of gynodioecy. *Trends in Ecology & Evolution* **22**: 17-24.

Dornier, A. & Dufay, M. 2013. How selfing, inbreeding depression, and pollen limitation impact nuclear-cytoplasmic gynodioecy: A model. *Evolution* **67**: 2674-2687.

Dufay, M., Touzet, P., Maurice, S. & Cuguen, J. 2007. Modelling the maintenance of male-fertile cytoplasm in a gynodioecious population. *Heredity* **99**: 349-356.

Fisher, R. A. 1941. Average excess and average effect of a gene substitution. *Annals of Eugenics* **11**: 53-63.

Frank, S. A. 1989. The evolutionary dynamics of cytoplasmic male-sterility. *American Naturalist* **133**: 345-376.

Geritz, S. A. H., Kisdi, E., Meszena, G. & Metz, J. A. J. 1998. Evolutionarily singular strategies and the adaptive growth and branching of the evolutionary tree. *Evolutionary Ecology* **12**: 35-57.

Goodwillie, C., Kalisz, S. & Eckert, C. G. 2005. The evolutionary enigma of mixed mating systems in plants: Occurrence, theoretical explanations, and empirical evidence. *Annual Review of Ecology Evolution and Systematics* **36**: 47-79.

Gouyon, P. H., Vichot, F. & Vandamme, J. M. M. 1991. Nuclear-cytoplasmic male-sterility - single-point equilibria versus limit-cycles. *American Naturalist* **137**: 498-514.

Hanson, M. R. 1991. Plant mitochondrial mutations and male-sterility. *Annual Review of Genetics* **25**: 461-486.

Harder, L. D. & Wilson, W. G. 1998. A clarification of pollen discounting and its joint effects with inbreeding depression on mating system evolution. *American Naturalist* **152**: 684-695.

Jacobs, M. S. & Wade, M. J. 2003. A synthetic review of the theory of gynodioecy. *American Naturalist* **161**: 837-851.

Johnston, M. O. 1998. Evolution of intermediate selfing rates in plants: pollination ecology versus deleterious mutations. *Genetica* **102-3**: 267-278.

Knight, T. M., Steets, J. A., Vamosi, J. C., Mazer, S. J., Burd, M., Campbell, D. R., Dudash, M. R., Johnston, M. O., Mitchell, R. J. & Ashman, T. L. 2005. Pollen limitation of plant reproduction: Pattern and process. *Annual Review of Ecology Evolution and Systematics* **36**: 467-497.

Lahiani, E., Touzet, P., Billard, E. & Dufay, M. 2015. When is it worth being a self-compatible hermaphrodite? Context-dependent effects of self-pollination on female advantage in gynodioecious Silene nutans. *Ecology and Evolution* **5**: 1854-1862.

Lande, R. & Schemske, D. W. 1985. The evolution of self-fertilization and inbreeding depression in plants .1. Genetic models. *Evolution* **39**: 24-40.

Lewis, D. 1941. Male sterility in natural populations of hermaphrodite plants. *New Phytologist* **40**: 56–63.

Lloyd, D. G. 1974. Theoretical sex-ratios of dioecious and gynodioecious angiosperms. *Heredity* **32**: 11-34.

Lloyd, D. G. 1975. Maintenance of gynodioecy and androdioecy in angiosperms. *Genetica* **45**: 325-339.

Lloyd, D. G. 1976. Transmission of genes via pollen and ovules in gynodioecious angiosperms. *Theoretical Population Biology* **9**: 299-316.

Lloyd, D. G. 1979. Some reproductive factors affecting the selection of self-fertilization in plants. *American Naturalist* **113**: 67-79.

Maurice, S., Charlesworth, D., Desfeux, C., Couvet, D. & Gouyon, P. H. 1993. The evolution of gender in hermaphrodites of gynodioecious populations with nucleocytoplasmic male-sterility. *Proceedings of the Royal Society B-Biological Sciences* **251**: 253-261.

Maurice, S. & Fleming, T. H. 1995. The effect of pollen limitation on plant reproductive systems and the maintenance of sexual polymorphisms. *Oikos* **74**: 55-60.

McCauley, D. E. & Bailey, M. F. 2009. Recent advances in the study of gynodioecy: the interface of theory and empiricism. *Annals of Botany* **104**: 611-620.

Parker, M. A. 1994. Pathogens and Sex in Plants. *Evolutionary Ecology* **8**: 560-584.

Porcher, E. & Lande, R. 2005a. The evolution of self-fertilization and inbreeding depression under pollen discounting and pollen limitation. *Journal of Evolutionary Biology* **18**: 497-508.

Porcher, E. & Lande, R. 2005b. Reproductive compensation in the evolution of plant mating systems. *New Phytologist* **166**: 673-684.

Sicard, A. & Lenhard, M. 2011. The selfing syndrome: a model for studying the genetic and evolutionary basis of morphological adaptation in plants. *Annals of Botany* **107**: 1433-1443.

Webb, C. L. (1999) Empirical studies: evolution and maintenance of dimorphic breeding systems. In: *Gender and sexual dimorphism in flowering plants*, (Geber, M. A., Dawson, T. E. & Delph, L. F., eds.). pp. 61-95. Springer, Berlin.

FIGURE CAPTIONS

Figure 1. Feasible and stable equilibria and evolutionarily realized selfing rates in the case that restorer cost reduces male function (cost type 1). Parameter μ is the cost of restorer, and 1 - δ is the inbreeding coefficient. Initially, the equilibria are analyzed under a given selfing rate. Depending on parameters, 5 types of equilibria are possible. An equilibrium with fixation of nuclear restorer, $(0, X_{Mn}, 0, X_{Mc})$, can be bistable with another equilibrium (regions that are surrounded by a broken curve). In the grayscale chart, characters represent sex determination modes of the population, NG: nuclear gynodioecy, CG: cytoplasmic gynodioecy, and NCG: nuclear-cytoplasmic gynodioecy. H1 and H2 represent hermaphroditic populations without CMS and restorer, and that with a fixation of restorer, respectively. It should be noted that the state H2 can be bistable with other equilibrium states depending on parameters. When H2 is a unique equilibrium, it is indicated by H2'. Subsequently, selfing evolution is examined under equilibrium states. Solid circles represent solutions that are both convergently and evolutionarily stable, whereas open circles are convergently unstable solutions, with given k values. See Table 1 for parameter values.

Figure 2. Feasible and stable equilibria and evolutionarily realized selfing rates in a case that a restorer cost reduces individual performance (cost type 2). Parameter μ is the cost of restorer, and 1 - δ is the inbreeding coefficient. Solid circles represent selfing rates that are both convergently and evolutionarily stable, whereas open circles are convergently unstable solutions. Parameters and conditions are identical to Fig. 1.

Figure 3. Simulation of the coevolution of CMS and nuclear restorer under a given selfing rate. Parameter values and conditions correspond to Fig. 1(e) with $k = 0.5$, in which equilibrium restorer-CMS status are bistability of $(0, X_{Mn}, 0, X_{Mc})$ (gray region on X_{Mn}-X_{Mc} axis) and another equilibrium, (1, 0, 0, 0) in (a), $(X_{mn}, 0, X_{mc}, 0)$ in (b) and $(X_{mn}, X_{Mn}, X_{mc}, X_{Mc})$ in (c). On the other hand, $(0, X_{Mn}, 0, X_{Mc})$ is

a unique equilibrium in (d). On the X_{Mn}-X_{Mc} axis, CMS mitochondria are neutral due to a fixation of nuclear restorer, although the equilibrium (0, X_{Mn}, 0, X_{Mc}) can be unstable when the CMS frequency goes below a threshold (small X_{Mc}). In (d), Genetic drift and subsequent emergence of non-restorer allele may cause cyclic dynamics.

Table 1 Notations of traits and parameters

	Description
Genotypic frequencies	
X_{mn}, X'_{mn}	non-restorer and non-CMS with resident and mutant selfing rate
X_{Mn}, X'_{Mn}	restorer and non-CMS with resident and mutant selfing rate
X_{mc}, X'_{mc}	non-restorer and CMS with resident and mutant selfing rate
X_{Mc}, X'_{Mc}	restorer and CMS with resident and mutant selfing rate
Quantitative genetic trait	
s, s'	resident and mutant selfing rate
Parameters and functions	
$D_p(s)$	pollen discounting: $1 - [b + (a - b)s^c]s$
a	reduction when $s = 1$, $0 \leq a \leq 1$ ($a = 1$ in numerical analysis)
b	concaveness of functional form ($b = 0$ in numerical analysis)
c	magnitude of curvature of functional form, $0 < c$ ($c = 0.5$ in numerical analysis)
$L_p(P_{EX})$	pollen limitation: $\beta P_{EX} / (\alpha + P_{EX})$
P_{EX}	density of exported pollen
α	extent of saturation ($\alpha = 0.1$ in numerical analysis)
β	maximum fertilization efficiency in outbreeding ($\beta = 1$ in numerical analysis)
r	recombination rate between restorer and selfing rate loci ($r = 0.5$ in simulation)
δ	inbreeding depression, $0 \leq \delta \leq 1$
η	$(1 - \delta) / \beta$, relative advantage of inbreeding to outbreeding
k	advantage of CMS in female performance (ovule production)
μ	cost accompanying with restorer allele, $0 \leq \mu \leq 1$

Table 2 Mating system, feasibility and stability conditions of equilibria in Eqs. (2) and (3).

Equilibrium	Mating system	Feasibility and stability conditions
Cost type 1		
(2a)	H	$\{(k-1)(1-s)-2s\eta\}(1-\mu)D_p(s) \leq 2s\alpha\eta$, and $X_{Mn} \leq 1 - \mu$
(2b)	NG	$0 < k(1-s) - s\eta$, and $\{(k-1)(1-s)-2s\eta\}(1-\mu)D_p(s) > 2s\alpha\eta$
(2c)	CG	$s\alpha\eta \leq \{k(1-s)-s\eta\}D_p(s) \leq s\alpha\eta\frac{1+k(1-\mu)}{(1+k)(1-\mu)}$
(2d)	NCG	$\frac{1+k(1-\mu)}{(1+k)(1-\mu)}s\alpha\eta < \{k(1-s)-s\eta\}D_p(s) < \frac{1}{1-\mu}s\alpha\eta$ (this is a feasibility condition, stability is numerically examined)
Cost type 2		
(3a)	H	$\left\{-\frac{(1-s)(1-2\mu-k)}{2(1-\mu)} - s\eta\right\}D_p(s) \leq s\alpha\eta \leq \left\{\frac{(1-s)(1-2\mu)}{2\mu} - s\eta\right\}D_p(s)$, and $X_{Mn} \leq \frac{-2s\alpha\eta\mu+\{(1-s)(1-2\mu)-2s\eta\mu\}D_p(s)}{(1-s)D_p(s)}$
(3b)	NG	$0 < (1-s)\{k(2-\mu)+\mu\} - 2s\eta(1-\mu)$, $s\alpha\eta \leq -\left\{\frac{(1-s)(1-k-2\mu)}{2(1-\mu)} + s\eta\right\}D_p(s)$, and $s\alpha\eta \leq \frac{(1+k)(1-\mu)}{2(k+\mu)}\{k(1-s)-2s\eta\}D_p(s)$
(3c)	CG	$s\alpha\eta \leq \{k(1-s)-s\eta\}D_p(s) \leq s\alpha\eta\frac{1+\mu}{1-\mu}$
(3d)	NCG	(both feasibility and stability are numerically examined)

H: hermaphrodite, NG: nuclear gynodioecy, CG: cytoplasmic gynodioecy, and NCG: nuclear-cytoplasmic gynodioecy

Table 3 Effects of parameters on instabilities of boundary selfing rates (see Eqs. (4)-(6)).

	cost type 1				cost type 2			
	$s = 0$			$s = 1$	$s = 0$			$s = 1$
	NG	H2’	H1	(H1)	NG	H2’	H1	(H1)
a	N/A	N/A	N/A	-	N/A	N/A	N/A	-
b	-	-	-	N/A	-	-	-	N/A
α	+	+	+	-	+	+	+	-
$\eta(= (1-\delta)/\beta)$	+	+	+	-	+	+	+	-
k	-	N/A	N/A	N/A	-	N/A	N/A	N/A
μ	+	+	N/A	N/A	-	N/A	N/A	N/A

NG: nuclear gynodioecy, H2’: hermaphrodite with (0, 0, 0, 1), H1: hermaphrodite with (1, 0, 0, 0), "+": promotion of instability, "-": suppression of instability, N/A: no effect

Figure 1

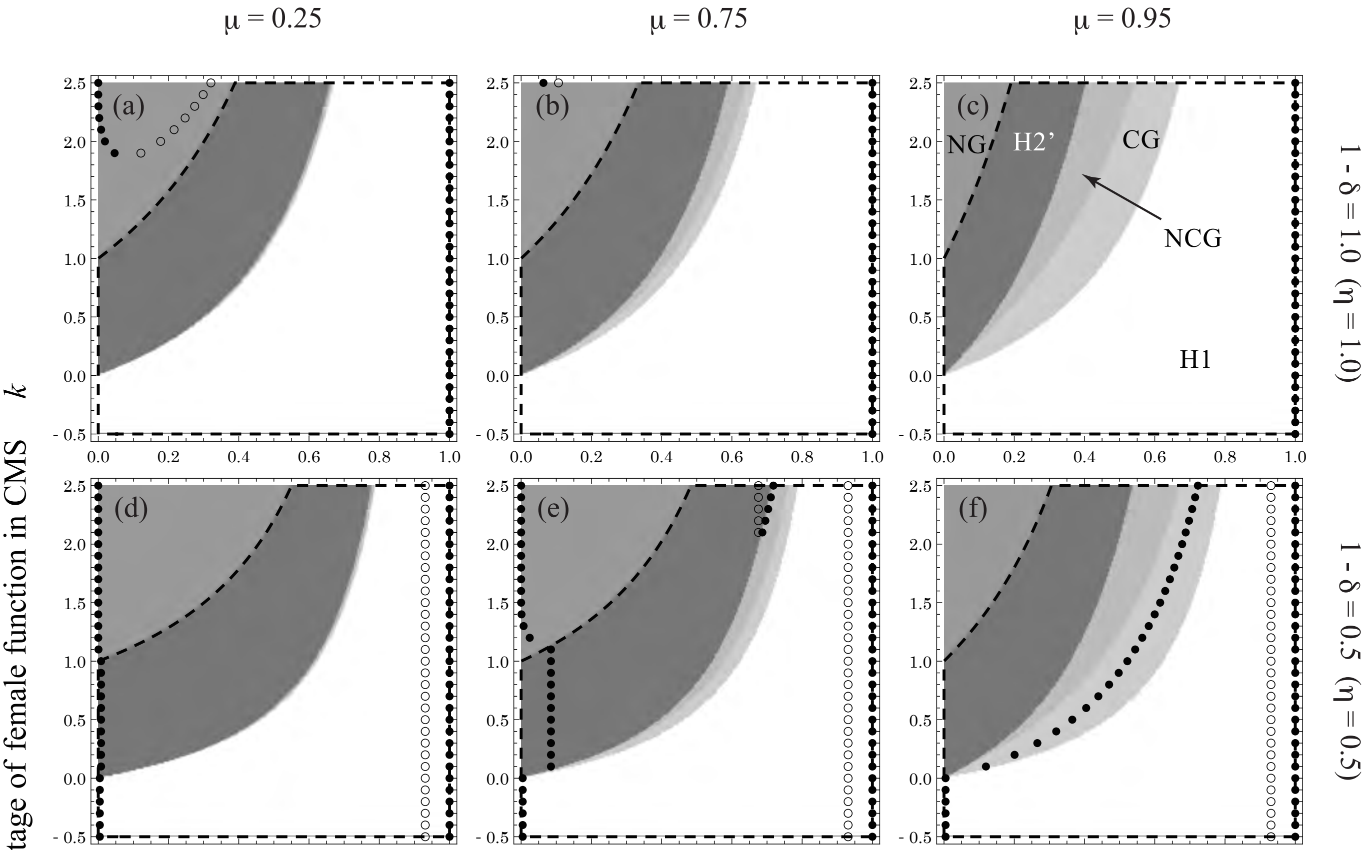
μ = 0.25
μ = 0.75
μ = 0.95
1 - δ = 1.0 (η = 1.0)
1 - δ = 0.5 (η = 0.5)
1 - δ = 0.25 (η = 0.25)
Advantage of female function in CMS k
Selfing rate s
(a)
(b)
(c)
(d)
(e)
(f)
(g)
(h)
(i)
NG
H2'
CG
NCG
H1
-0.5
0.0
0.5
1.0
1.5
2.0
2.5
0.0
0.2
0.4
0.6
0.8
1.0
NCG $(X_{mn}, X_{Mn}, X_{mc}, X_{Mc})$
CG $(X_{mn}, 0, X_{mc}, 0)$
H1 $(1, 0, 0, 0)$
H2 $(0, X_{Mn}, 0, X_{Mc})$
H2' $(0, X_{Mn}, 0, X_{Mc})$ only
NG $(0, 0, X_{mc}, X_{Mc})$ only

Figure 2

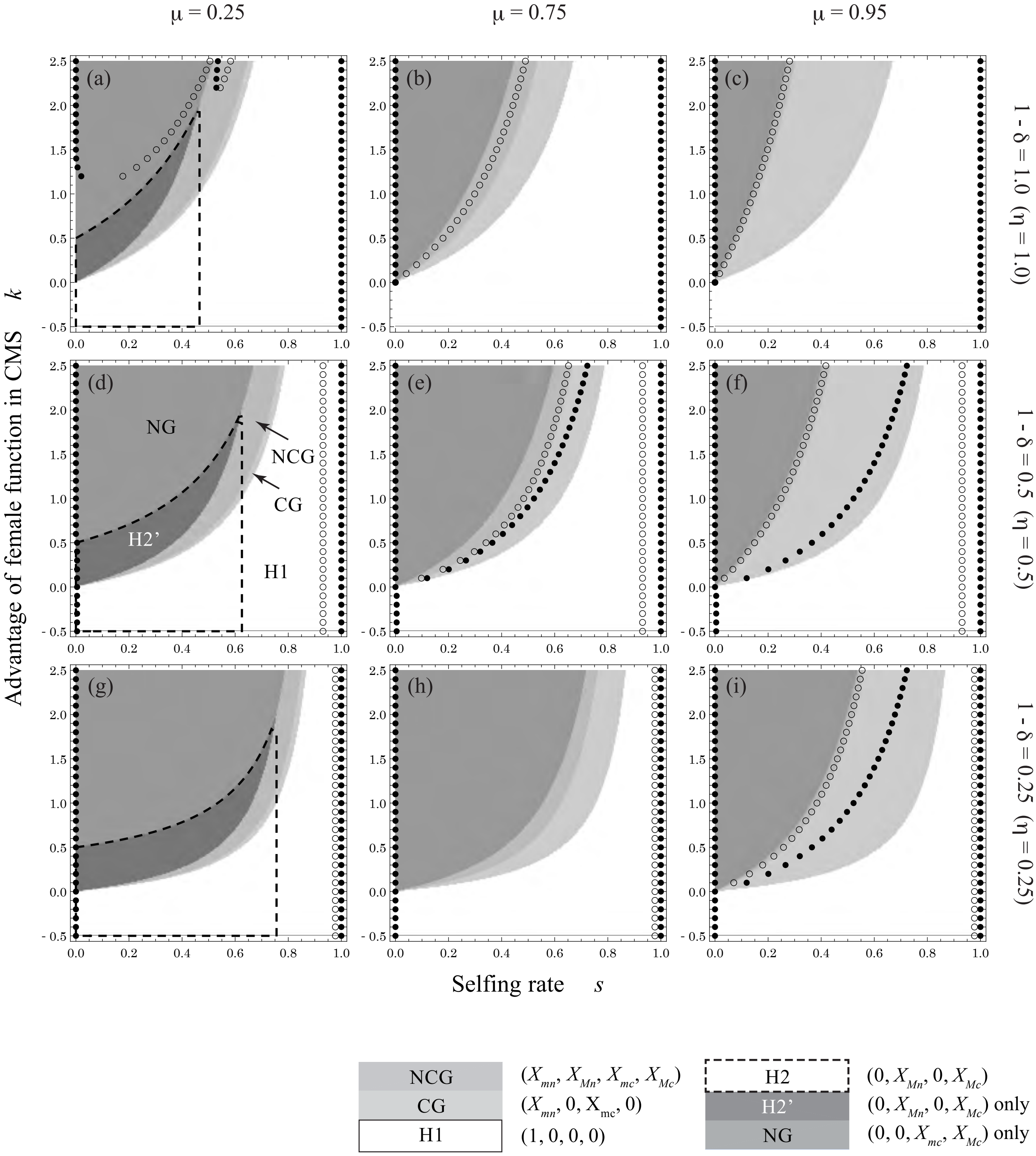
μ = 0.25
μ = 0.75
μ = 0.95
1 - δ = 1.0 (η = 1.0)
1 - δ = 0.5 (η = 0.5)
1 - δ = 0.25 (η = 0.25)
Advantage of female function in CMS k
Selfing rate s
(a)
(b)
(c)
(d)
(e)
(f)
(g)
(h)
(i)
NG
NCG
CG
H2'
H1
- 0.5
0.0
0.5
1.0
1.5
2.0
2.5
0.0
0.2
0.4
0.6
0.8
1.0
NCG $(X_{mn}, X_{Mn}, X_{mc}, X_{Mc})$
CG $(X_{mn}, 0, X_{mc}, 0)$
H1 $(1, 0, 0, 0)$
H2 $(0, X_{Mn}, 0, X_{Mc})$
H2' $(0, X_{Mn}, 0, X_{Mc})$ only
NG $(0, 0, X_{mc}, X_{Mc})$ only

Figure 3

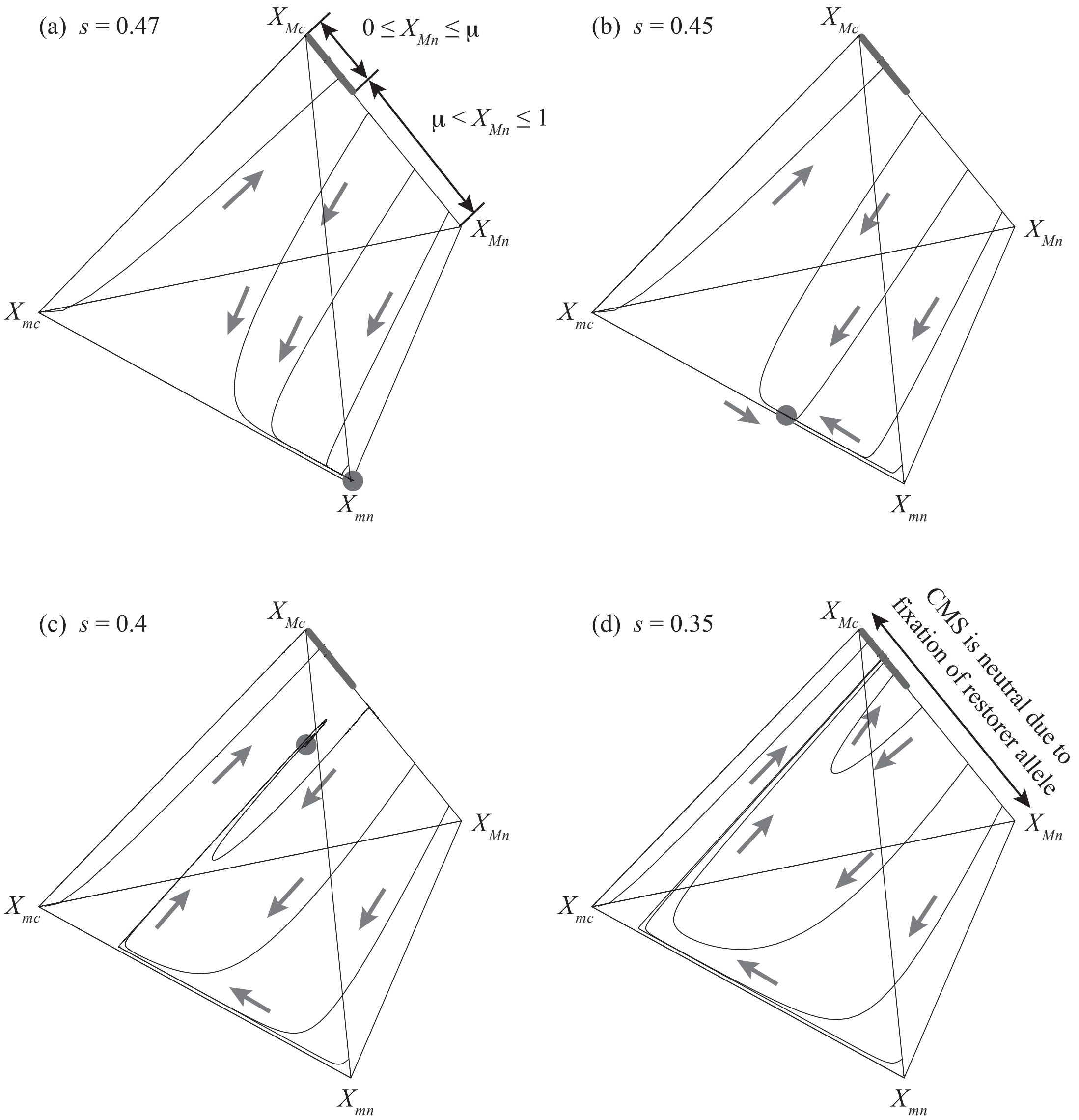
(a) $s = 0.47$
X_{Mc}
$0 \leq X_{Mn} \leq \mu$
$\mu < X_{Mn} \leq 1$
X_{Mn}
X_{mc}
X_{mn}
(b) $s = 0.45$
X_{Mc}
X_{Mn}
X_{mc}
X_{mn}
(c) $s = 0.4$
X_{Mc}
X_{Mn}
X_{mc}
X_{mn}
(d) $s = 0.35$
X_{Mc}
CMS is neutral due to
fixation of restorer allele
X_{Mn}
X_{mc}
X_{mn}

APPENDIX A

We formulate the dynamics of genotypic frequencies by combining the reproductive outcomes of selfing and outbreeding. It should be noted that outbreeding success is affected by the average density of exported pollen through both pollen limitation and pollen competition for ovules. For simplicity of description, we refer to X_{mn}, X_{Mn}, X_{mc}, X_{Mc}, X'_{mn}, X'_{Mn}, X'_{mc} and X'_{Mc} by w, x, y, z, w', x', y' and z' in this section. The offspring genotype in outbreeding between two genotypes is summarized in Supplementary Table 1.

Dynamic equation with cost type 1

First, we consider cost type 1 that the nuclear restorer reduces individual pollen production (in x_t, x'_t, z_t and z'_t), a fraction of which is denoted by μ. A relative amount of pollen that is exported by an individual decreases with its selfing rate, i.e., pollen discounting, which we denote as $D_p(s)$. On the other hand, the relative density of exported pollen in the population can be expressed by the average pollen exportation from individuals, which is formulated as $P_{EX} = \{w_t + (1-\mu)(x_t + z_t)\}D_p(s) + \{w'_t + (1-\mu)(x'_t + z'_t)\}D_p(s')$. It should be noted that CMS individuals without restorer (i.e., y_t and y'_t) cannot produce pollen at all, but promote ovule production with relative ratio k.

Frequencies dynamics of strains with a resident selfing rate s are

$$w_{t+1} = \llbracket (1-\delta)sw_t + \frac{\beta P_{EX}}{\alpha + P_{EX}}\Big[D_p(s)\Big\langle(1-s)\Big\{\frac{w_t}{P_{EX}}\Big(w_t + \frac{1}{2}x_t\Big) + (1-\mu)\frac{x_t + z_t}{P_{EX}}\frac{1}{2}w_t\Big\} +$$

$$(1-s')\Big\{\frac{w_t}{P_{EX}}\Big(\frac{1}{2}w'_t + \frac{1}{2}(1-r)x'_t\Big) + (1-\mu)\frac{x_t+z_t}{P_{EX}}\frac{1}{2}rw'_t\Big\}\Big\rangle +$$

$$D_p(s')(1-s)\Big\{\frac{w'_t}{P_{EX}}\Big(\frac{1}{2}w_t + \frac{1}{2}rx_t\Big) + (1-\mu)\frac{x'_t+z'_t}{P_{EX}}\frac{1}{2}rw_t\Big\}\Big]\rrbracket \frac{1}{W} \ ,$$

(A1a)

$$x_{t+1} = \Bigl\llbracket (1-\delta)sx_t + \frac{\beta P_{EX}}{\alpha + P_{EX}}\Bigl[D_p(s)\Bigl\langle(1-s)\Bigl\{\frac{w_t}{P_{EX}}\frac{1}{2}x_t + (1-\mu)\frac{x_t+z_t}{P_{EX}}\Bigl(\frac{1}{2}w_t + x_t\Bigr)\Bigr\} +$$

$$(1-s')\Bigl\{\frac{w_t}{P_{EX}}\frac{1}{2}rx'_t + (1-\mu)\frac{x_t+z_t}{P_{EX}}\Bigl(\frac{1}{2}(1-r)w'_t + \frac{1}{2}x'_t\Bigr)\Bigr\}\Bigr\rangle +$$

$$D_p(s')(1-s)\Bigl\{\frac{w'_t}{P_{EX}}\frac{1}{2}(1-r)x_t + (1-\mu)\frac{x'_t+z'_t}{P_{EX}}\Bigl(\frac{1}{2}rw_t + \frac{1}{2}x_t\Bigr)\Bigr\}\Bigr]\Bigr\rrbracket\frac{1}{W} \ ,$$

(A1b)

$$y_{t+1} = \frac{\beta P_{EX}}{\alpha + P_{EX}}\Bigl[D_p(s)\Bigl\langle(1-s)\Bigl\{\frac{w_t}{P_{EX}}\Bigl((1+k)y_t + \frac{1}{2}z_t\Bigr) + (1-\mu)\frac{x_t+z_t}{P_{EX}}(1+k)\frac{1}{2}y_t\Bigr\} +$$

$$(1-s')\Bigl\{\frac{w_t}{P_{EX}}\Bigl((1+k)\frac{1}{2}y'_t + \frac{1}{2}(1-r)z'_t\Bigr) + (1-\mu)\frac{x_t+z_t}{P_{EX}}(1+k)\frac{1}{2}rw'_t\Bigr\}\Bigr\rangle +$$

$$D_p(s')(1-s)\Bigl\{\frac{w'_t}{P_{EX}}\Bigl((1+k)\frac{1}{2}y_t + \frac{1}{2}rz_t\Bigr) + (1-\mu)\frac{x'_t+z'_t}{P_{EX}}(1+k)\frac{1}{2}ry_t\Bigr\}\Bigr]\frac{1}{W} \ ,$$

(A1c)

$$z_{t+1} = \llbracket(1-\delta)sz_t +$$

$$\frac{\beta P_{EX}}{\alpha+P_{EX}}\Bigl[D_p(s)\Bigl\langle(1-s)\Bigl\{\frac{w_t}{P_{EX}}\frac{1}{2}z_t + (1-\mu)\frac{x_t+z_t}{P_{EX}}\Bigl((1+k)\frac{1}{2}y_t + z_t\Bigr)\Bigr\} +$$

$$(1-s')\Bigl\{\frac{w_t}{P_{EX}}\frac{1}{2}rz'_t + (1-\mu)\frac{x_t+z_t}{P_{EX}}\Bigl((1+k)\frac{1}{2}(1-r)y'_t + \frac{1}{2}z'_t\Bigr)\Bigr\}\Bigr\rangle +$$

$$D_p(s')(1-s)\Bigl\{\frac{w'_t}{P_{EX}}\frac{1}{2}(1-r)z_t + (1-\mu)\frac{x'_t+z'_t}{P_{EX}}\Bigl((1+k)\frac{1}{2}ry_t + \frac{1}{2}z_t\Bigr)\Bigr\}\Bigr]\Bigr\rrbracket\frac{1}{W} \ ,$$

(A1d)

whereas those with a mutant selfing rate *s*' are

$$w'_{t+1} = \llbracket(1-\delta)s'w'_t +$$

$$\frac{\beta P_{EX}}{\alpha+P_{EX}}\Bigl[D_p(s)(1-s')\Bigl\{\frac{w_t}{P_{EX}}\Bigl(\frac{1}{2}w'_t + \frac{1}{2}rx'_t\Bigr) + (1-\mu)\frac{x_t+z_t}{P_{EX}}\frac{1}{2}(1-r)w'_t\Bigr\} +$$

$$D_p(s')\Bigl\langle(1-s)\Bigl\{\frac{w'_t}{P_{EX}}\Bigl(\frac{1}{2}w_t + \frac{1}{2}(1-r)x_t\Bigr) + (1-\mu)\frac{x'_t+z'_t}{P_{EX}}\frac{1}{2}rw_t\Bigr\} +$$

$$(1-s')\Bigl\{\frac{w'_t}{P_{EX}}\Bigl(w'_t + \frac{1}{2}x'_t\Bigr) + (1-\mu)\frac{x'_t+z'_t}{P_{EX}}\frac{1}{2}w'_t\Bigr\}\Bigr\rangle\Bigr]\Bigr\rrbracket\frac{1}{W} \ ,$$

(A1e)

$$x'_{t+1} = \Big[\!\Big[(1-\delta)s'x'_t +$$

$$\frac{\beta P_{EX}}{\alpha+P_{EX}}\Big[D_p(s)(1-s')\Big\{\frac{w_t}{P_{EX}}\frac{1}{2}(1-r)x'_t + (1-\mu)\frac{x_t+z_t}{P_{EX}}\Big(\frac{1}{2}rw'_t + \frac{1}{2}x'_t\Big)\Big\} +$$

$$D_p(s')\Big\langle(1-s)\Big\{\frac{w'_t}{P_{EX}}\frac{1}{2}rx_t + (1-\mu)\frac{x'_t+z'_t}{P_{EX}}\Big(\frac{1}{2}(1-r)w_t + \frac{1}{2}x_t\Big)\Big\} +$$

$$(1-s')\Big\{\frac{w'_t}{P_{EX}}\frac{1}{2}x'_t + (1-\mu)\frac{x'_t+z'_t}{P_{EX}}\Big(\frac{1}{2}w'_t + x'_t\Big)\Big\}\Big\rangle\Big]\Big]\!\Big]\frac{1}{W} \;,$$

(A1f)

$$y'_{t+1} =$$

$$\frac{\beta P_{EX}}{\alpha+P_{EX}}\Big[D_p(s)(1-s')\Big\{\frac{w_t}{P_{EX}}\Big((1+k)\frac{1}{2}y'_t + \frac{1}{2}rz'_t\Big) + (1-\mu)\frac{x_t+z_t}{P_{EX}}(1+k)\frac{1}{2}(1-r)y'_t\Big\} +$$

$$D_p(s')\Big\langle(1-s)\Big\{\frac{w'_t}{P_{EX}}\Big((1+k)\frac{1}{2}y_t + \frac{1}{2}(1-r)z_t\Big) + (1-\mu)\frac{x'_t+z'_t}{P_{EX}}(1+k)\frac{1}{2}ry_t\Big\} +$$

$$(1-s')\Big\{\frac{w'_t}{P_{EX}}\Big((1+k)y'_t + \frac{1}{2}z'_t\Big) + (1-\mu)\frac{x'_t+z'_t}{P_{EX}}(1+k)\frac{1}{2}y'_t\Big\}\Big\rangle\Big]\frac{1}{W} \;,$$

(A1g)

$$z'_{t+1} = \Big[\!\Big[(1-\delta)s'z'_t +$$

$$\frac{\beta P_{EX}}{\alpha+P_{EX}}\Big[D_p(s)(1-s')\Big\{\frac{w_t}{P_{EX}}\frac{1}{2}(1-r)z'_t + (1-\mu)\frac{x_t+z_t}{P_{EX}}\Big((1+k)\frac{1}{2}ry'_t + \frac{1}{2}z'_t\Big)\Big\} +$$

$$D_p(s')\Big\langle(1-s)\Big\{\frac{w'_t}{P_{EX}}\frac{1}{2}rz_t + (1-\mu)\frac{x'_t+z'_t}{P_{EX}}\Big((1+k)\frac{1}{2}(1-r)y_t + \frac{1}{2}z_t\Big)\Big\} +$$

$$(1-s')\Big\{\frac{w'_t}{P_{EX}}\frac{1}{2}z'_t + (1-\mu)\frac{x'_t+z'_t}{P_{EX}}\Big((1+k)\frac{1}{2}y'_t + z'_t\Big)\Big\}\Big\rangle\Big]\Big]\!\Big]\frac{1}{W} \;.$$

(A1h)

In these equations, W represents the average fitness.

Dynamic equation with cost type 2

Next, we consider cost type 2 that the nuclear restorer reduces individual performance (in x_t, x'_t, z_t

and z'_t). This cost is assumed to reduce individual survivorship immediately before the census timing of genotypic frequencies, a fraction of which is denoted by μ. The relative density of exported pollen in the population can be expressed by the average pollen exportation from individuals, which can be formulated as $P_{EX} = \{w_t + (x_t + z_t)\}D_p(s) + \{w'_t + (x'_t + z'_t)\}D_p(s')$.

Similarly to the previous case, frequencies of genotypes with a resident selfing rate s are expressed as

$$\begin{aligned} w_{t+1} = {} & [\![(1-\delta)sw_t + \frac{\beta P_{EX}}{\alpha + P_{EX}}\left[D_p(s)\left\langle (1-s)\left\{\frac{w_t}{P_{EX}}\left(w_t + \frac{1}{2}x_t\right) + \frac{x_t+z_t}{P_{EX}}\frac{1}{2}w_t\right\} + \right.\right. \\ & \left.\left. (1-s')\left\{\frac{w_t}{P_{EX}}\left(\frac{1}{2}w'_t + \frac{1}{2}(1-r)x'_t\right) + \frac{x_t+z_t}{P_{EX}}\frac{1}{2}rw'_t\right\}\right\rangle + \right. \\ & \left. D_p(s')(1-s)\left\{\frac{w'_t}{P_{EX}}\left(\frac{1}{2}w_t + \frac{1}{2}rx_t\right) + \frac{x'_t+z'_t}{P_{EX}}\frac{1}{2}rw_t\right\}\right]]\!] \frac{1}{W} \ , \end{aligned} \tag{A2a}$$

$$\begin{aligned} x_{t+1} = {} & (1-\mu) [\![(1-\delta)sx_t + \frac{\beta P_{EX}}{\alpha + P_{EX}}\left[D_p(s)\left\langle (1-s)\left\{\frac{w_t}{P_{EX}}\frac{1}{2}x_t + \frac{x_t+z_t}{P_{EX}}\left(\frac{1}{2}w_t + x_t\right)\right\} + \right.\right. \\ & \left.\left. (1-s')\left\{\frac{w_t}{P_{EX}}\frac{1}{2}rx'_t + \frac{x_t+z_t}{P_{EX}}\left(\frac{1}{2}(1-r)w'_t + \frac{1}{2}x'_t\right)\right\}\right\rangle + \right. \\ & \left. D_p(s')(1-s)\left\{\frac{w'_t}{P_{EX}}\frac{1}{2}(1-r)x_t + \frac{x'_t+z'_t}{P_{EX}}\left(\frac{1}{2}rw_t + \frac{1}{2}x_t\right)\right\}\right]]\!] \frac{1}{W} \ , \end{aligned} \tag{A2b}$$

$$\begin{aligned} y_{t+1} = {} & \frac{\beta P_{EX}}{\alpha + P_{EX}}\frac{1}{P_{EX}}\left[D_p(s)\left\langle (1-s)\left\{\frac{w_t}{P_{EX}}\left((1+k)y_t + \frac{1}{2}z_t\right) + \frac{x_t+z_t}{P_{EX}}(1+k)\frac{1}{2}y_t\right\} + \right.\right. \\ & \left.\left. (1-s')\left\{\frac{w_t}{P_{EX}}\left((1+k)\frac{1}{2}y'_t + \frac{1}{2}(1-r)z'_t\right) + \frac{x_t+z_t}{P_{EX}}(1+k)\frac{1}{2}rw'_t\right\}\right\rangle + \right. \\ & \left. D_p(s')(1-s)\left\{\frac{w'_t}{P_{EX}}\left((1+k)\frac{1}{2}y_t + \frac{1}{2}rz_t\right) + \frac{x'_t+z'_t}{P_{EX}}(1+k)\frac{1}{2}ry_t\right\}\right] \frac{1}{W} \ , \end{aligned} \tag{A2c}$$

$$
\begin{aligned}
z_{t+1} = (1-\mu)\llbracket(1-\delta)sz_t + {} \\
\frac{\beta P_{EX}}{\alpha+P_{EX}}\Big[D_p(s)\Big\langle(1-s)\Big\{\frac{w_t}{P_{EX}}\frac{1}{2}z_t + \frac{x_t+z_t}{P_{EX}}\Big((1+k)\frac{1}{2}y_t + z_t\Big)\Big\} + {} \\
(1-s')\Big\{\frac{w_t}{P_{EX}}\frac{1}{2}rz'_t + \frac{x_t+z_t}{P_{EX}}\Big((1+k)\frac{1}{2}(1-r)y'_t + \frac{1}{2}z'_t\Big)\Big\}\Big\rangle + {} \\
D_p(s')(1-s)\Big\{\frac{w'_t}{P_{EX}}\frac{1}{2}(1-r)z_t + \frac{x'_t+z'_t}{P_{EX}}\Big((1+k)\frac{1}{2}ry_t + \frac{1}{2}z_t\Big)\Big\}\Big]\rrbracket\frac{1}{W} \quad ,
\end{aligned}
$$

(A2d)

whereas those with a mutant selfing rate *s*' are

$$
\begin{aligned}
w'_{t+1} = \llbracket(1-\delta)s'w'_t + {} \\
\frac{\beta P_{EX}}{\alpha+P_{EX}}\Big[D_p(s)(1-s')\Big\{\frac{w_t}{P_{EX}}\Big(\frac{1}{2}w'_t + \frac{1}{2}rx'_t\Big) + \frac{x_t+z_t}{P_{EX}}\frac{1}{2}(1-r)w'_t\Big\} + {} \\
D_p(s')\Big\langle(1-s)\Big\{\frac{w'_t}{P_{EX}}\Big(\frac{1}{2}w_t + \frac{1}{2}(1-r)x_t\Big) + \frac{x'_t+z'_t}{P_{EX}}\frac{1}{2}rw_t\Big\} + {} \\
(1-s')\Big\{\frac{w'_t}{P_{EX}}\Big(w'_t + \frac{1}{2}x'_t\Big) + \frac{x'_t+z'_t}{P_{EX}}\frac{1}{2}w'_t\Big\}\Big\rangle\Big]\rrbracket\frac{1}{W} \quad ,
\end{aligned}
$$

(A2e)

$$
\begin{aligned}
x'_{t+1} = (1-\mu)\llbracket(1-\delta)s'w'_t + {} \\
\frac{\beta P_{EX}}{\alpha+P_{EX}}\Big[D_p(s)(1-s')\Big\{\frac{w_t}{P_{EX}}\frac{1}{2}(1-r)x'_t + \frac{x_t+z_t}{P_{EX}}\Big(\frac{1}{2}rw'_t + \frac{1}{2}x'_t\Big)\Big\} + {} \\
D_p(s')\Big\langle(1-s)\Big\{\frac{w'_t}{P_{EX}}\frac{1}{2}rx_t + \frac{x'_t+z'_t}{P_{EX}}\Big(\frac{1}{2}(1-r)w_t + \frac{1}{2}x_t\Big)\Big\} + {} \\
(1-s')\Big\{\frac{w'_t}{P_{EX}}\frac{1}{2}x'_t + \frac{x'_t+z'_t}{P_{EX}}\Big(\frac{1}{2}w'_t + x'_t\Big)\Big\}\Big\rangle\Big]\rrbracket\frac{1}{W} \quad ,
\end{aligned}
$$

(A2f)

$$
\begin{aligned}
y'_{t+1} = \frac{\beta P_{EX}}{\alpha+P_{EX}}\Big[D_p(s)(1-s')\Big\{\frac{w_t}{P_{EX}}\Big((1+k)\frac{1}{2}y'_t + \frac{1}{2}rz'_t\Big) + \frac{x_t+z_t}{P_{EX}}(1+k)\frac{1}{2}(1-r)y'_t\Big\} + {} \\
D_p(s')\Big\langle(1-s)\Big\{\frac{w'_t}{P_{EX}}\Big((1+k)\frac{1}{2}y_t + \frac{1}{2}(1-r)z_t\Big) + \frac{x'_t+z'_t}{P_{EX}}(1+k)\frac{1}{2}ry_t\Big\} + {} \\
(1-s')\Big\{\frac{w'_t}{P_{EX}}\Big((1+k)y'_t + \frac{1}{2}z'_t\Big) + \frac{x'_t+z'_t}{P_{EX}}(1+k)\frac{1}{2}y'_t\Big\}\Big\rangle\Big]\frac{1}{W} \quad ,
\end{aligned}
$$

(A2g)

$$
\begin{aligned}
z'_{t+1} = {} & (1-\mu)[\![(1-\delta)s'w'_t + \\
& \frac{\beta P_{EX}}{\alpha+P_{EX}}\Big[D_p(s)(1-s')\Big\{\frac{w_t}{P_{EX}}\frac{1}{2}(1-r)z'_t + \frac{x_t+z_t}{P_{EX}}\Big((1+k)\frac{1}{2}ry'_t + \frac{1}{2}z'_t\Big)\Big\} + \\
& D_p(s')\Big\langle(1-s)\Big\{\frac{w'_t}{P_{EX}}\frac{1}{2}rz_t + \frac{x'_t+z'_t}{P_{EX}}\Big((1+k)\frac{1}{2}(1-r)y_t + \frac{1}{2}z_t\Big)\Big\} + \\
& (1-s')\Big\{\frac{w'_t}{P_{EX}}\frac{1}{2}z'_t + \frac{x'_t+z'_t}{P_{EX}}\Big((1+k)\frac{1}{2}y'_t + z'_t\Big)\Big\}\Big\rangle\Big]]\!]\frac{1}{W} \;.
\end{aligned}
$$

(A2h)

In these equations, W represents the average fitness.

APPENDIX B

Invasibility of mutant selfing rate

We consider invasions of s - 10^{-8} and s + 10^{-8} mutant selfing rates into a resident mutation rate s, dominant eigenvalues of which are denoted by λ_- and λ_+, respectively. The mutant can increase in the population when a norm of the dominant eigenvalue $\|\lambda\|$ is greater than 1. Therefore, the trait value evolves towards a larger value when $\|\lambda_-\| \leq 1$ and $\|\lambda_+\| > 1$ (i.e., $\|\lambda_-\| \leq 1 < \|\lambda_+\|$), and towards a lower value when $\|\lambda_-\| > 1$ and $\|\lambda_+\| \leq 1$ (i.e., $\|\lambda_-\| > 1 \geq \|\lambda_+\|$). Since the norm of the dominant eigenvalue of a resident selfing rate s itself is always 1, these conditions can be simplified as $\|\lambda_-\| < \|\lambda_+\|$ and $\|\lambda_-\| > \|\lambda_+\|$, respectively, during the transient process towards an evolutionary singular point. Accordingly, we search for interior convergently stable selfing rates by looking for changing points of sign $\|\lambda_+\| - \|\lambda_-\|$ from positive to negative by using a bisection method for a value of s. We also examine the evolutionary stability of those solutions, in which a resident selfing rate can be stable if both $\|\lambda_+\| \leq 1$ and $\|\lambda_-\| \leq 1$ hold simultaneously. On the other hand, boundaries s = 0 and s = 1 can be convergently and evolutionarily stable solutions when neighborhoods of those boundaries satisfy $\|\lambda_+\| - \|\lambda_-\| < 0$ and $\|\lambda_+\| - \|\lambda_-\| > 0$, respectively.

PIP of selfing evolution

We plot PIP with examinations of mutant invasibility by using the same procedure as above, although the interval of selfing is set to 0.005 rather than 10^{-8} to reduce the calculation load. Supplementary figures 1 and 2 represent PIP for $k = 1$ cases of Figs. 1 and 2, respectively. A grayscale chart above each panel indicates a mating mode under the given resident selfing rate, which corresponds to grayscale in Figs. 1 and 2. In those figures, the gray regions indicate a successful invasion of a rare mutant strategy (a coordinate of the vertical axis) into the population of resident strategy (a coordinate of the horizontal axis), while the white regions represent the failure of mutant invasion. On the diagonal line, the mutant strategy coincides with the resident strategy. When the plot is white both above and below a point on the diagonal line, it indicates that mutants with slightly larger and smaller values of strategies than the resident strategy cannot increase in the resident population, implying evolutionary stability of the resident strategy. In those figures, solid circles represent convergently and evolutionarily stable states, whereas open circles are convergently unstable states (as Figs. 1 and 2). According to the figures, we can graphically reconfirm evolutionary stabilities of equilibria that are indicated by the solid circles.

Interestingly, in Supplementary figure 1(i), a range of selfing rates can be continuously evolutionarily stable, which is indicated by the region with a black arrow. This seems inconsistent to Fig. 1(i), although it may result from the difference of mutation interval between the two figures. In the PIP, we set an interval of mutation at 0.005, which is smaller than that of the above numerical analysis, 10^{-8}. The larger interval in PIP results in a range of selfing rates that are continuously evolutionarily stable. Indeed, an examination with a smaller interval of selfing rate (i.e., 10^{-8}) suggests that the boundary of invasibility adjoins the diagonal line, implying that the evolutionarily stable selfing rate is a point rather than a region.

CAPTIONS OF SUPPLEMENTARY FIGURES

Supplementary Figure 1. Pairwise invasibility plot (PIP) of selfing rate. Each panel indicates a PIP under the same condition as a corresponding panel of Fig. 1 with $k = 1$. Solid circles represent selfing rates that are both convergently and evolutionarily stable, whereas open circles are convergently unstable solutions. A grayscale chart above each panel indicates a mating mode under the given resident selfing rate, which correspond to grayscale in Fig. 1. In panel (i), an arrow indicates a region where a certain range of selfing rates are continuously evolutionary stable (see Appendix B).

Supplementary Figure 2. Pairwise invasibility plot (PIP) of selfing rate. Each panel indicates a PIP under the same condition as a corresponding panel of Fig. 2 with $k = 1$. Solid circles represent selfing rates that are both convergently and evolutionarily stable, whereas open circles are convergently unstable solutions. A grayscale chart above each panel indicates a mating mode under the given resident selfing rate, which correspond to grayscale in Fig. 2.

Supplementary Figure 3. Feasible and stable equilibria and evolutionarily realized selfing rates in a case that a restorer cost reduces male function (cost type 1), with varying parameters of pollen limitation function, α and β. Solid circles represent selfing rates that are both convergently and evolutionarily stable, whereas open circles are convergently unstable solutions. In this figure, $\mu = 0.75$ and $1 - \delta = 0.75$, other parameters are shown in Table 1. The panels (b), (e), and (h) of this figure represent similar results to Figs. 1(h), (e) and (b), respectively, because of correspondences between μ, α and η ($= (1 - \delta)/\beta$) values, i.e., $\eta = 0.25$, 0.5 and 1.0.

Supplementary Figure 4. Feasible and stable equilibria and evolutionarily realized selfing rates in a case that a restorer cost reduces individual performance (cost type 2), with varying parameters of pollen limitation function, α and β. Parameters and conditions are identical to

Supplementary Fig. 3. The panels (b), (e), and (h) of this figure represent similar results with Figs. 2(h), (e) and (b), respectively, because of correspondences between μ, α and η (= (1 - δ)/β) values, i.e., η = 0.25, 0.5 and 1.0.

Supplementary Figure 5. Pairwise invasibility plot (PIP) of selfing rate. Each panel indicates a PIP under the same condition as a corresponding panel of Supplementary Fig. 3 with k = 1. Solid circles represent selfing rates that are both convergently and evolutionarily stable, whereas open circles are convergently unstable solutions. A grayscale chart above each panel indicates a mating mode under the given resident selfing rate, which corresponds to grayscale in Supplementary Fig. 3.

Supplementary Figure 6. Pairwise invasibility plot (PIP) of selfing rate. Each panel indicates a PIP under the same condition as a corresponding panel of Supplementary Fig. 4 with k = 1. Parameters and conditions are identical to Supplementary Fig. 4.

Supplementary Figure 7. Feasible and stable equilibria and evolutionarily realized selfing rates in a case that a restorer cost reduces male function (cost type 1), with varying parameters of pollen discounting function, a and b. Solid circles represent selfing rates that are both convergently and evolutionarily stable, whereas open circles are convergently unstable solutions. In this figure, μ = 0.75 and 1 - δ = 0.5, other parameters are shown in Table 1. Panel (i) of this figure corresponds to Fig. 1(e) due to identical parameters.

Supplementary Figure 8. Feasible and stable equilibria and evolutionarily realized selfing rates in a case that a restorer cost reduces individual performance (cost type 2), with varying parameters of pollen discounting function, a and b. Parameters and conditions are identical to Supplementary Fig. 7. The panel (i) of this figure corresponds to Fig. 2(e) due to identical parameters.

Supplementary Figure 9. Pairwise invasibility plot (PIP) of selfing rate. Each panel indicates a PIP under the same condition as a corresponding panel of Supplementary Fig. 7 with $k = 1$. Solid circles represent selfing rates that are both convergently and evolutionarily stable, whereas open circles are convergently unstable solutions. A grayscale chart above each panel indicates a mating mode under the given resident selfing rate, which corresponds to grayscale in Supplementary Fig. 7.

Supplementary Figure 10. Pairwise invasibility plot (PIP) of selfing rate. Each panel indicates a PIP under the same condition as a corresponding panel of Supplementary Fig. 8 with $k = 1$. Parameters and conditions are identical to Supplementary Fig. 8.

Supplementary Table 1 Mating table of outbreeding

					normal mitochondria				CMS mitochndria			
					wildtype selfing		mutant selfing		wildtype selfing		mutant selfing	
					w	x	w'	x'	y (female)	z	y' (female)	z'
				pollen\ovule	ms/n	Ms/n	ms'/n	Ms'/n	ms/c	Ms/c	ms'/c	Ms'/c
normal mitochondria	wildtype selfing	Dp(s)	w	ms	w:1	w:1/2 x:1/2	w:1/2 w':1/2	w:1/2(1−r) w':1/2r x':1/2(1−r) x:1/2r	y:1	y:1/2 z:1/2	y:1/2 y':1/2	y:1/2(1−r) y':1/2r z':1/2(1−r) z:1/2r
			x	Ms	w:1/2 x:1/2	x:1	w':1/2(1−r) w:1/2r x:1/2(1−r) x':1/2r	x:1/2 x':1/2	y:1/2 z:1/2	z:1	y':1/2(1−r) y:1/2r z:1/2(1−r) z':1/2r	z:1/2 z':1/2
	mutant selfing	Dp(s')	w'	ms'	w:1/2 w':1/2	w':1/2(1−r) w:1/2r x:1/2(1−r) x':1/2r	w':1	w':1/2 x':1/2	y:1/2 y':1/2	y':1/2(1−r) y:1/2r z:1/2(1−r) z':1/2r	y':1	y':1/2 z':1/2
			x'	Ms'	w:1/2(1−r) w':1/2r x':1/2(1−r) x:1/2r	x:1/2 x':1/2	w':1/2 x':1/2	x':1	y:1/2(1−r) y':1/2r z':1/2(1−r) z:1/2r	z:1/2 z':1/2	y':1/2 z':1/2	z':1
CMS mitochndria	wildtype selfing	Dp(s)	y									
			z	ms	w:1/2 x:1/2	x:1	w':1/2(1−r) w:1/2r x:1/2(1−r) x':1/2r	x1:1/2 x':1/2	y:1/2 z:1/2	z:1	y':1/2(1−r) y:1/2r z:1/2(1−r) z':1/2r	z:1/2 z':1/2
	mutant selfing	Dp(s')	y'									
			z'	Ms'	w:1/2(1−r) w':1/2r x':1/2(1−r) x:1/2r	x:1/2 x':1/2	w':1/2 x':1/2	x':1	y:1/2(1−r) y':1/2r z':1/2(1−r) z:1/2r	z:1/2 z':1/2	y':1/2 z':1/2	z':1

† Rows with the same color represet the sama mating consequence

Supplementary Figure 1

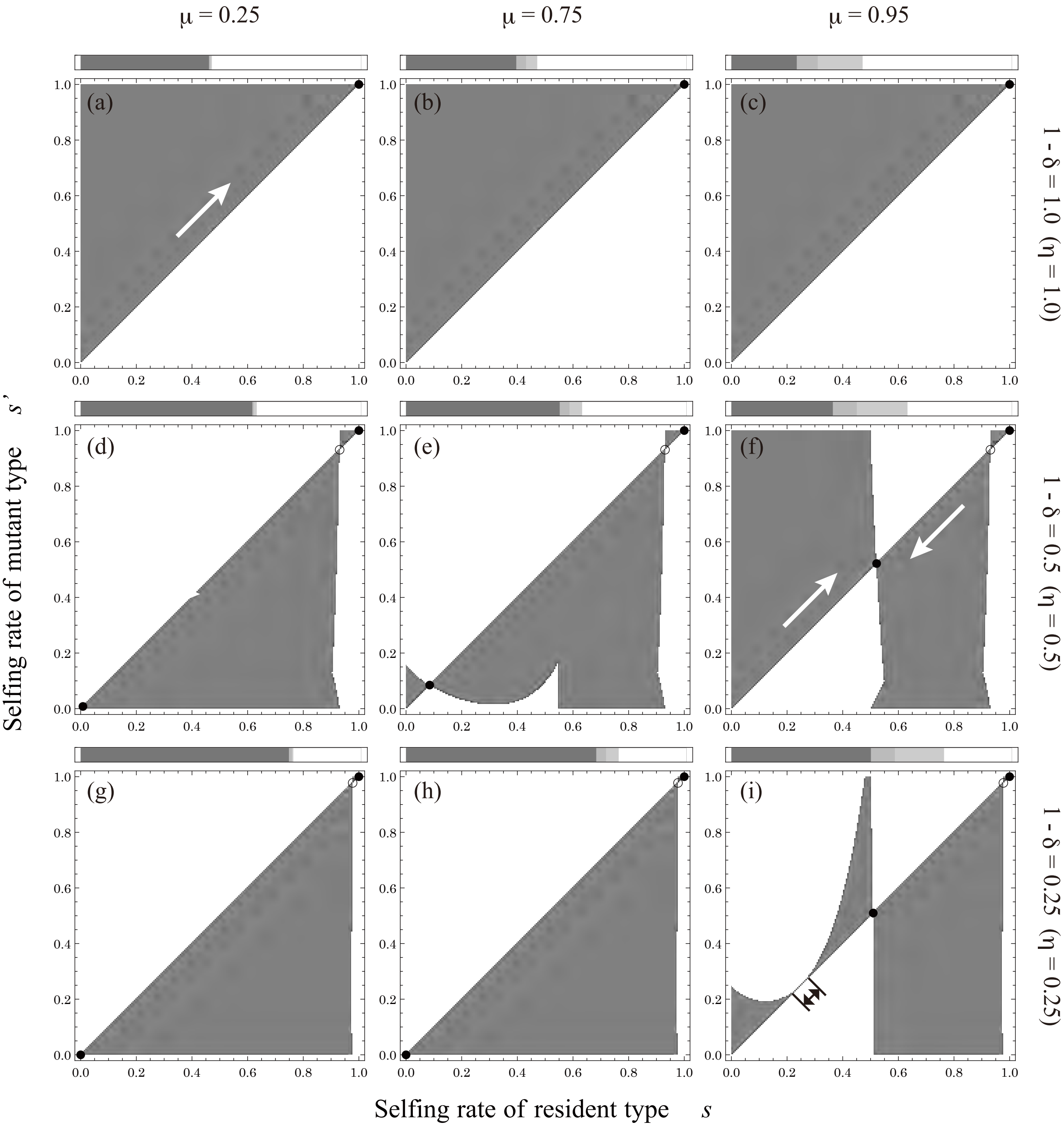

Supplementary Figure 2

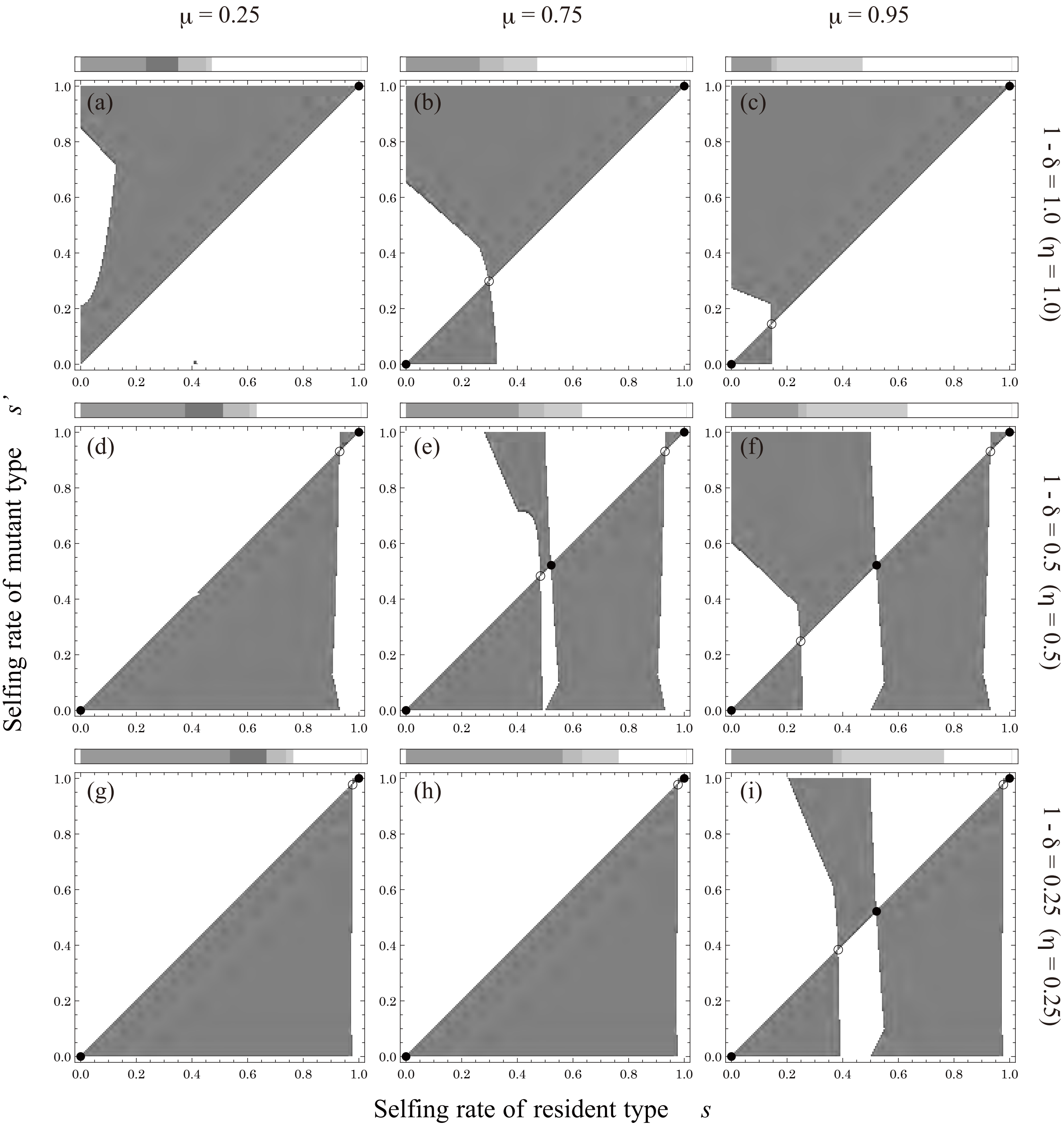

Supplementary Figure 3

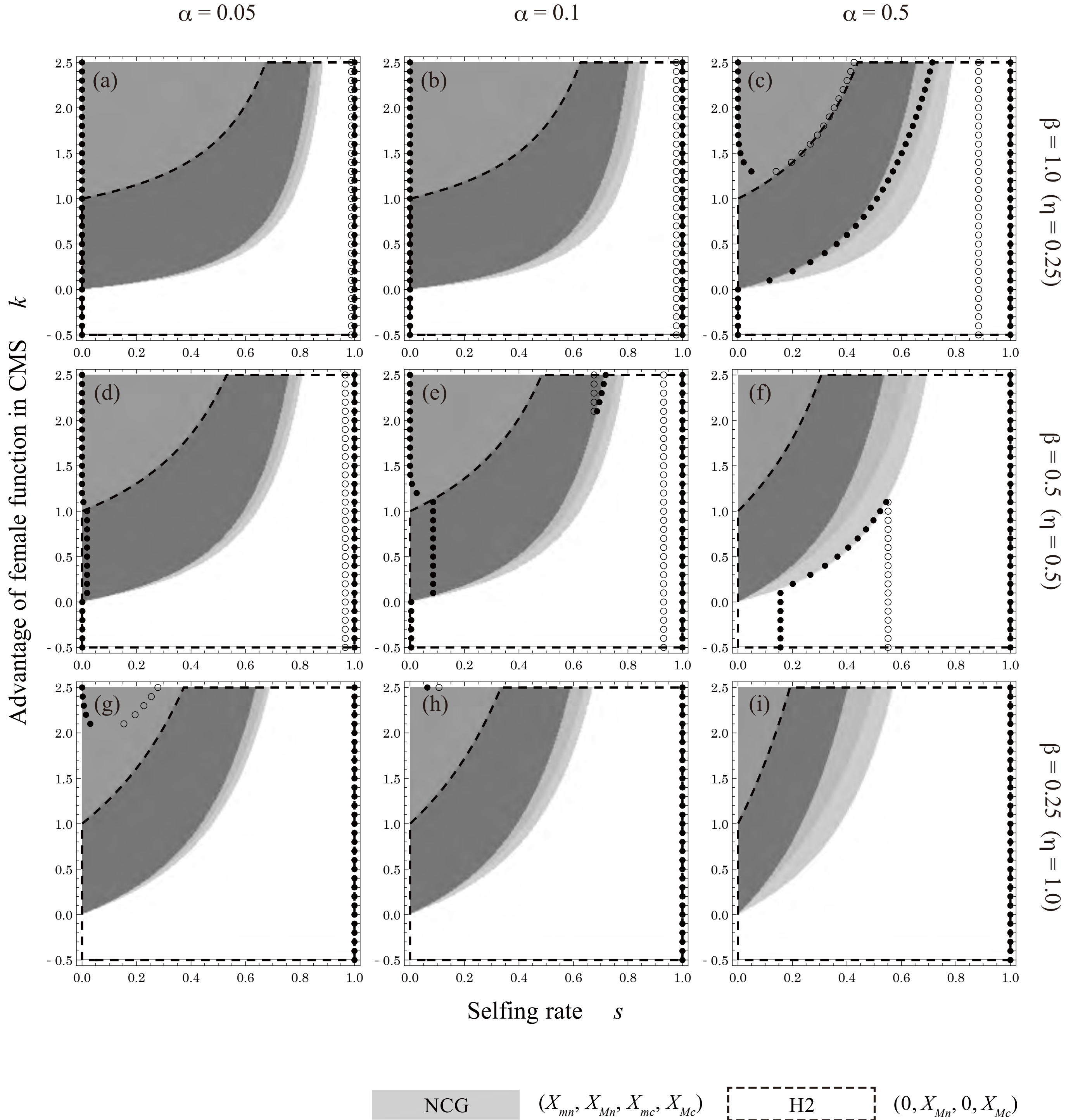

Supplementary Figure 4

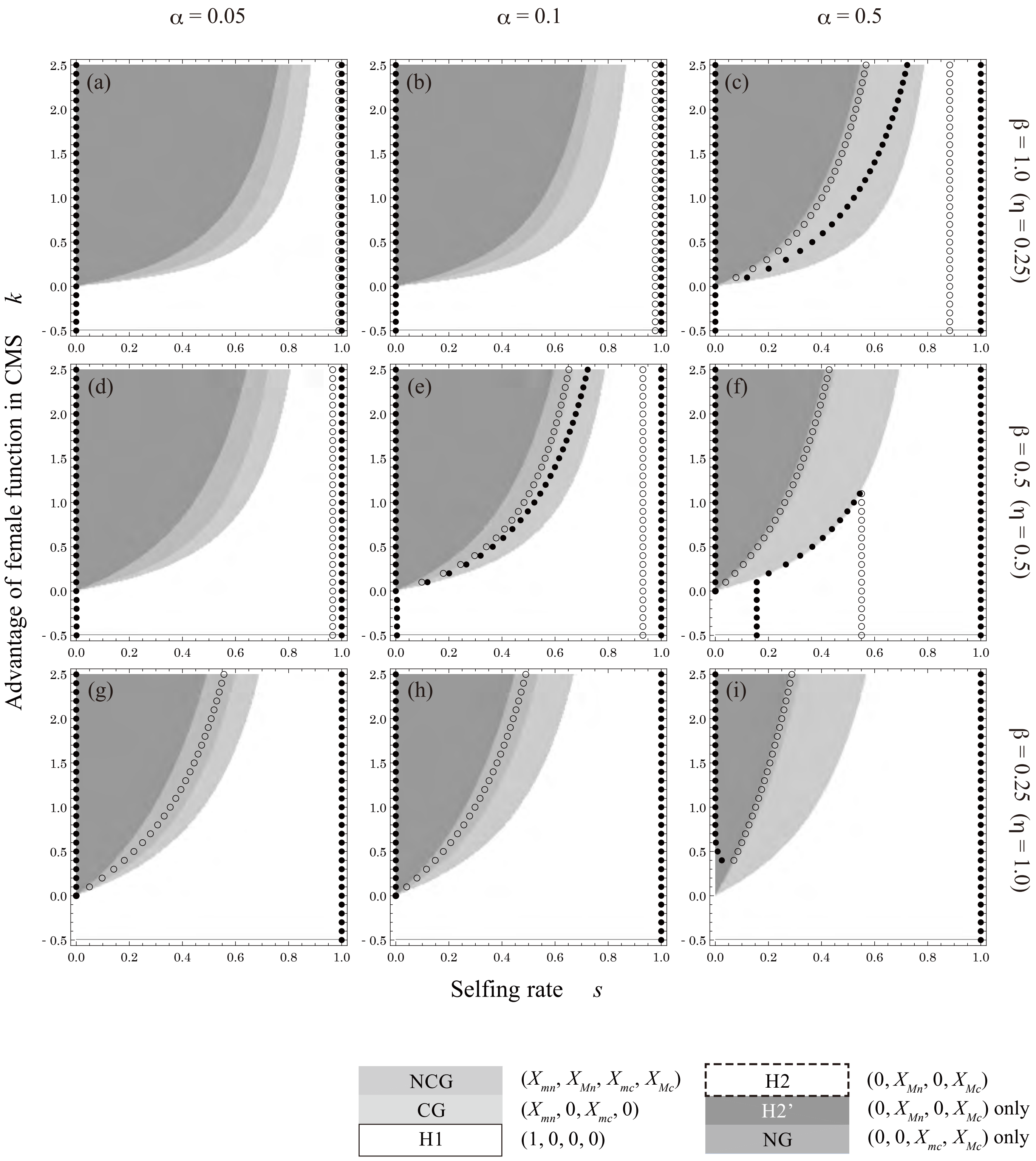

Supplementary Figure 5

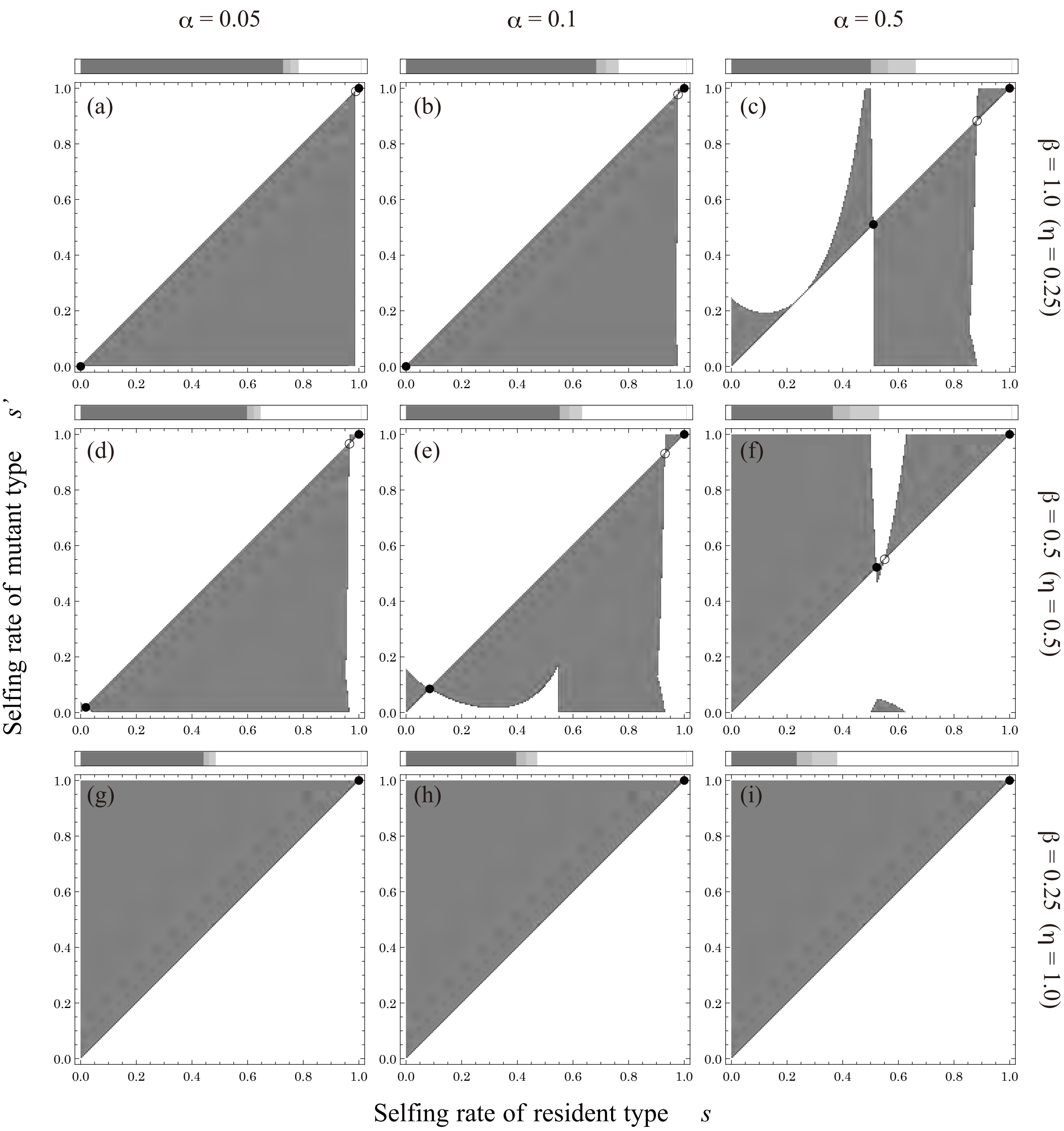

Supplementary Figure 6

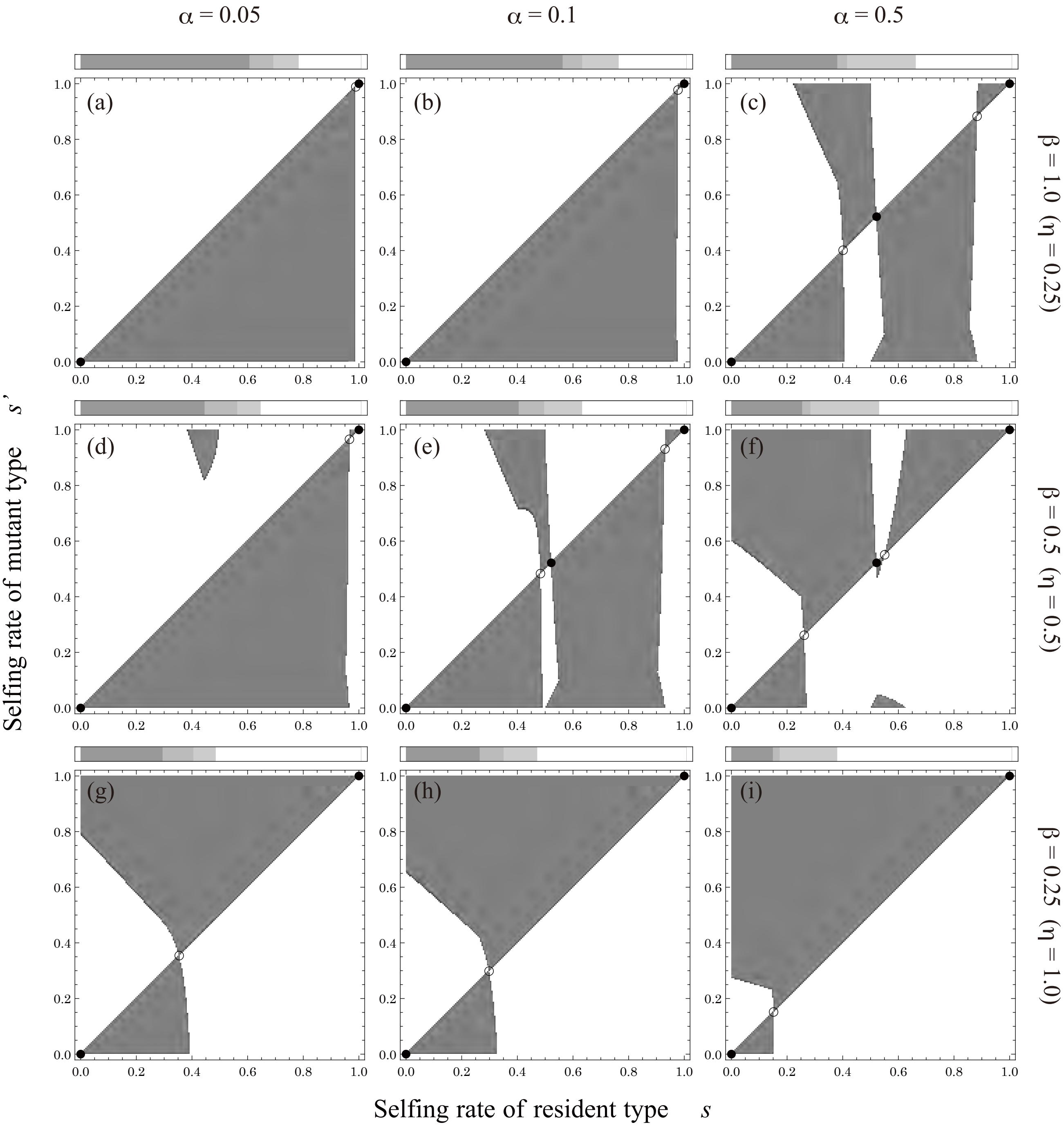

Supplementary Figure 7

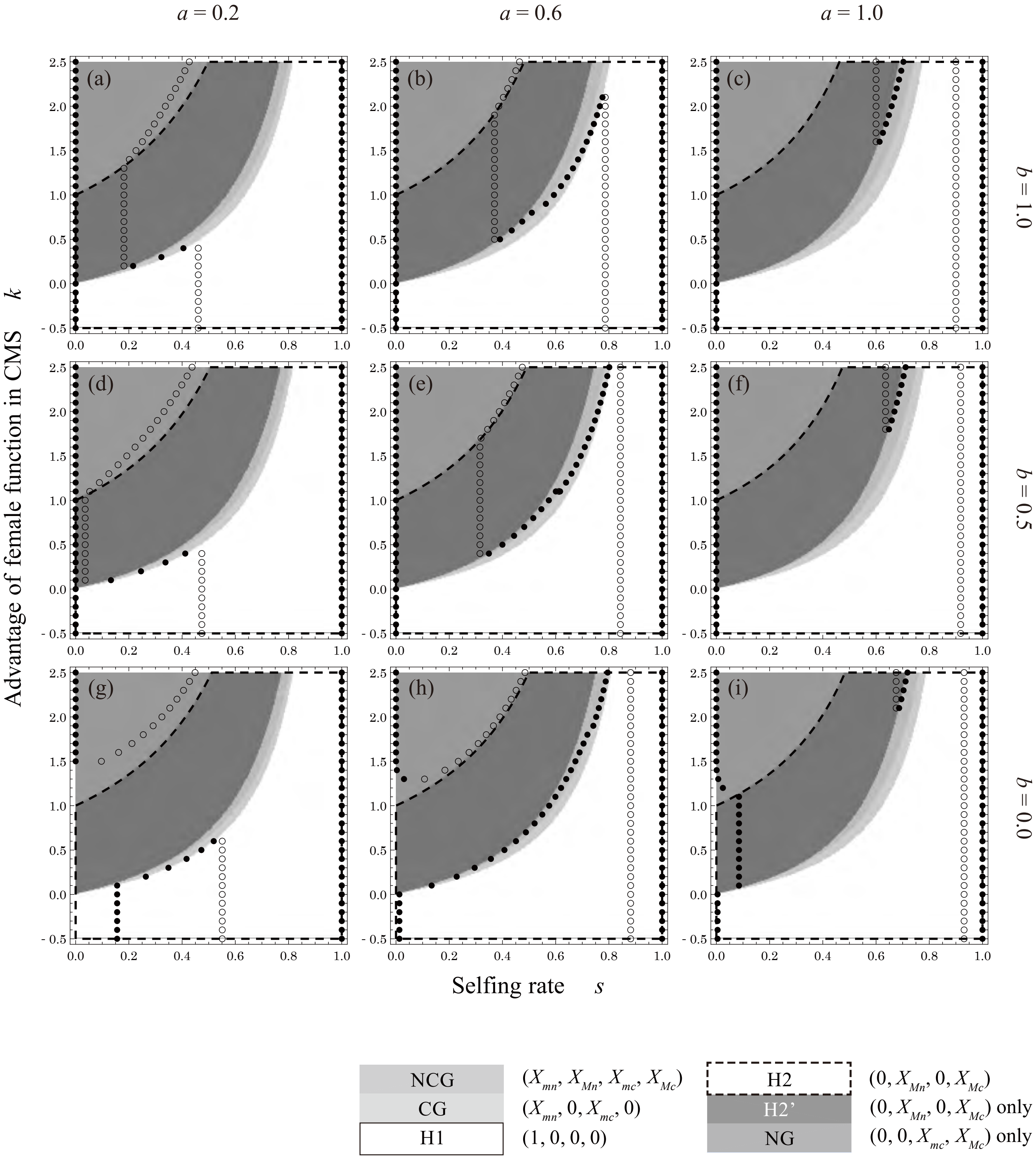

Supplementary Figure 8

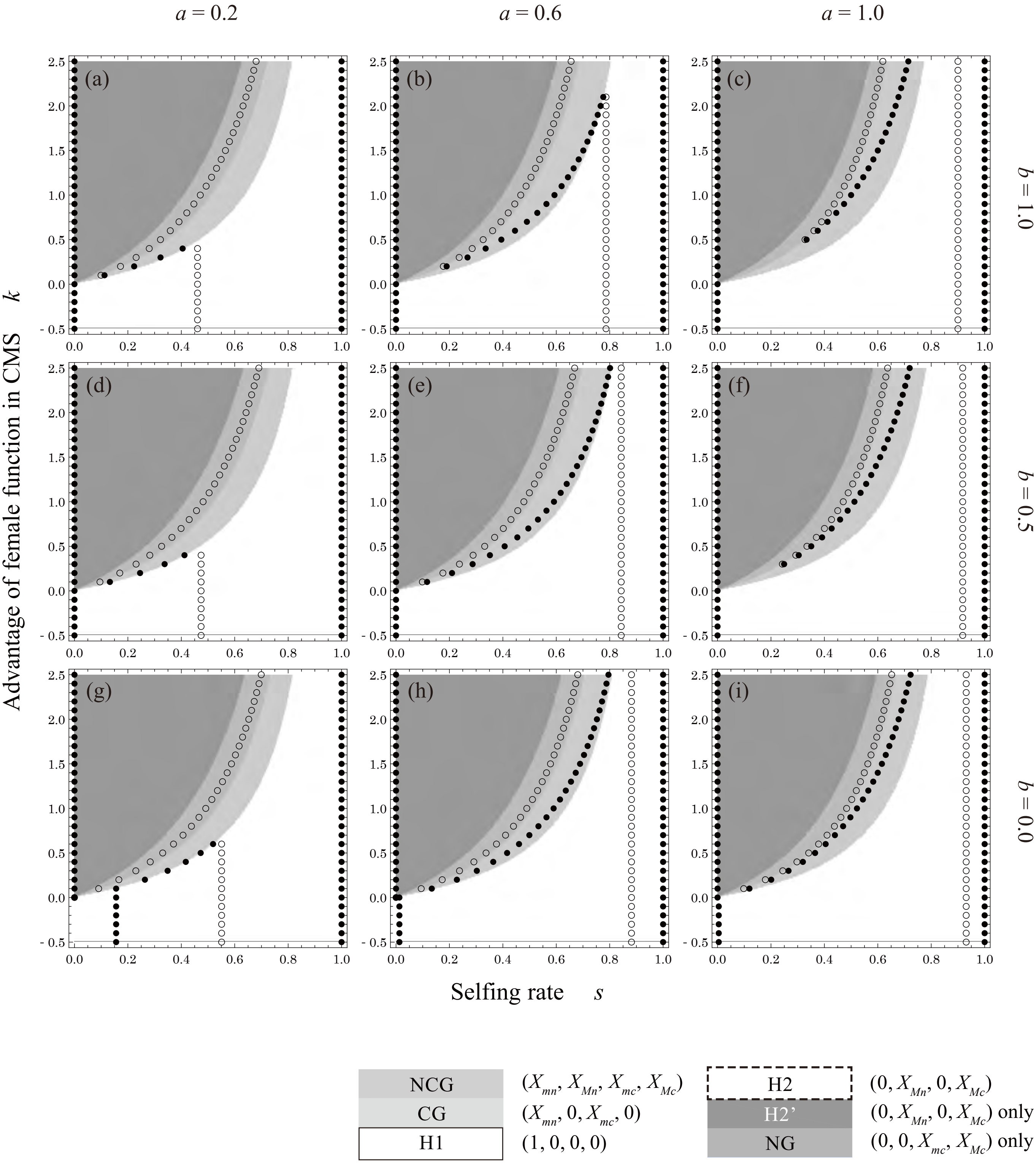

Supplementary Figure 9

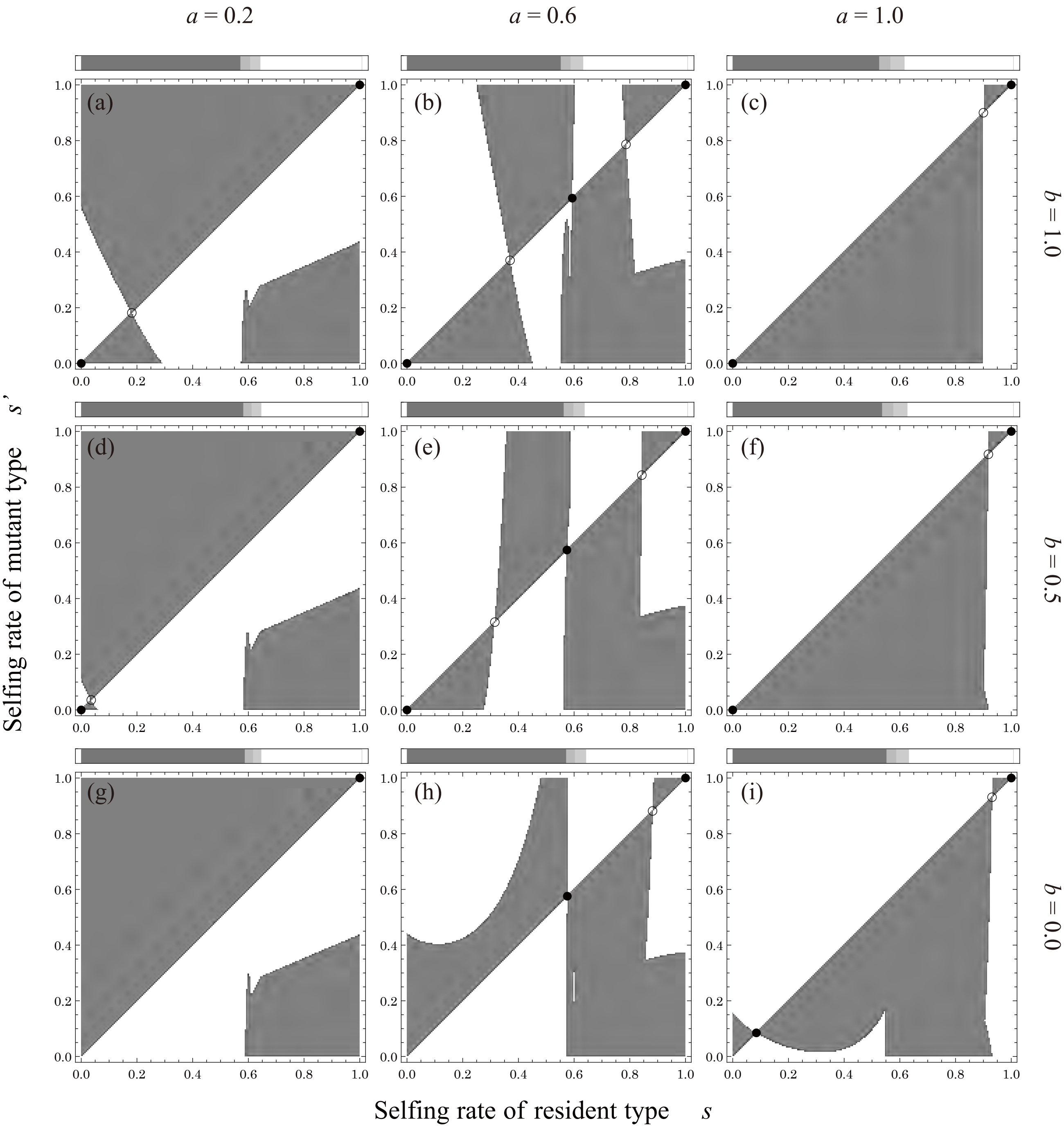

Supplementary Figure 10